Selective Detection and Removal of Mercury Ion by Dual-Functionalized Metal-Organic Frameworks: Design-for-Purpose

Leili Esrafili[a‡], Maniya Gharib[a‡], Ali Morsali[a]*

[a]Department of Chemistry, Faculty of Sciences, TarbiatModares University, P.O. Box 14115-175, Tehran, Iran. E-mail: Morsali_a@modares.ac.ir; Telephone: 0098-21-82884416, Cell Phone: 0098-9122420568

[‡]L.E. and M.Gh. contributed equally to this work.

1. Experimental Section

Materials and Characterization

All chemical reagents used in this work obtained from commercial suppliers, and used as received without further purification. Infrared spectra were recorded using Thermo Scientific Nicolet IR 100 FT-IR spectrometer. X-ray powder diffraction (XRD) measurements were done by a Philips X'pert diffractometer with mono chromated Cu-Kα radiation. Nitrogen sorption–desorption isotherms were obtained at 77 K on a TriStar II 3020 surface area analyzer from Micromeritics analyzer. Thermal curves were obtained on a PL-STA 1500 apparatus with the heating rate of 10ºC /min up to 800 ºC under a constant flow of nitrogen. Elemental analyses were collected on a CHNS Thermo Scientific Flash 2000 elemental analyzer. ^{1}H NMR spectra were recorded on a Bruker 500 MHz NMR spectrometer. Concentration of metal ions were analyzed by simultaneous inductively coupled plasma optical emission spectrometry (ICP-OES) on a Varian Vista-PRO instrument.

1.1. Synthesis of the ligands

1.1.1. Synthesis of bpta, bpfb and bpfn

The simple route for the synthesis of amide-containing compounds is the coupling of an acid chloride with an amine group. Note here that the acid chloride-amine reaction is exothermic. Therefore, all organic reactions performed in this study were carried out at low temperature in the presence of triethylamine (TEA) to capture in situ the generated side product HCl. Synthesis of bpta 4-aminopyridine (1.882 g; 20 mmol) and 2.84 ml of TEA (20.4 mmol) were dissolved in 50 ml of dry THF. Then, terephthaloyl chloride (2.030 g; 10 mmol) was added into this solution and heated under reflux for 24 h. The resulting yellow

suspension was filtered, dried under ambient conditions, and poured into an aqueous saturated solution of Na_2CO_3 (50 ml). The resulting white solid was finally filtered and dried, obtaining the pure ligand bpta in ca. 73 % yield.

Synthesis of bpfb and bpfn

1,5-diaminonaphthalene (1.580 g; 10 mmol; for bpfn) and 1,4-phenylenediamine (1.081 g; 10 mmol; for bpfb) were dissolved in 50 ml of dry THF containing 2.84 ml of TEA (20.4 mmol). Then, isonicotinoyl chloride hydrochloride (3.560 g, 20 mmol) was added into these solutions and heated under reflux for 24 h. Both reactions were then treated as above indicated for the synthesis of bpta. The yellowish powders were filtered and dried, obtaining the pure ligands in ca. 82 % (bpfb) and 87 % (bpfn) yields.

Synthesis of the ligand N1, N3-di(pyridine-4-yl) malonamide (S2)

The S2 spacer was synthesized by mixture of 0.07gr malonyl dichloride (0.5mmol) and 0.09gr of 4-amino pyridine (1mmol) in 40cc dry THF. After adding 8cc TEA (Triethylamine), put the mixture be refluxed in Ar condition for 24h.The resulting brown suspension was filtered, dried under ambient conditions, and poured into an aqueous saturated solution of Na2CO3 (50 ml). The resulting light brown solid was finally filtered and dried, obtaining the pure ligand S2 in ca. 73 % yield.

X-Ray Crystallography

The single-crystal diffraction data for TMU-46was collected on a Bruker AXS smart Apex CCD diffractometer at 296 K. The X-ray generator was operated at 50 kV and 35 mA using Mo-Ka (l 0.71073A °) radiation. The crystal structures were solved and refined by full matrix least-squares methods against F2 by using the program SHELXL-2014 using the Olex-2 software. All Non-hydrogen atoms were refined with anisotropic displacement parameters and hydrogen positions were fixed at calculated positions and refined isotopically. Crystallographic data and other pertinent information for compounds TMU-46 is summarized in Table S1.

CCDC numbers is 1849865 for compound TMU-46. More details on the crystallographic structures are presented in the Supplementary Material. Table S1

Activation Method

The trapped guest molecules can be removed by exchanging the synthesized parent crystals (TMU-46), (TMU-47) and (TMU-48) and daughter crystals (TMU-C46S), (TMU-47S) and (TMU-48S) With soaked MOFs in 3 mL of acetonitrile solvent for 2 days, and added fresh acetonitrile every 24 h. At last, the CH_3CN solution was decanted, and the activated crystals were dried at 100 °C for at least 24 h. The activation is confirmed by FT-IR spectroscopy, elemental analysis, and powder X-ray diffraction. Absence of the peak at 1665-1670 cm^{-1} in the FT-IR spectrum of parent and daughter activated samples confirms the removal of DMF molecules after activation.

FT-IR data (KBr pellet, cm-1): selected bands: 3359 (w), 2929 (w), 1599 (s), 1518 (s), 1382 (m), 1303 (w), 1182 (m), 1022 (w), 841 (w), 783 (w), 535 (w).

NMR of parent MOFs and SALE samples

Approximately 5 mg of each MOF was placed in an NMR tube and dissolved in 100 μL of D_2SO_4 and 0.6 mL of d6DMSO by sonication. Once a homogeneous solution was obtained, the ^1H NMR spectra were obtained.

Computational details

All DFT calculations were performed using the GAMESS suite of programs. The geometry of the ligands was optimized at the B3LYP/6-31+G* level of theory. The LANL2DZ basis set with the corresponding effective core potential was used for the metal cations. Molecular electrostatic potentials (MEPs) of the isolated ligand were obtained on the 0.001 au surface by means of the SAS-WFA program using the wave functions generated at the aforementioned level of theory. The Mulliken charge density analysis of the free ligands was performed at the B3LYP/6-31+G* level using the GAMESS.

Luminescence sensing procedure for Metal Ions

The luminescence sensing experiments were first accomplished as follows: 3 mg parent samples of TMU-46, 47 and 48 and the daughter samples of them (the respective weight) were ground and immersed in an aqueous solution of M^{x+} (M= Hg, Ag, Cu, Cd, Pb and Cr) (3 mL) with a different concentration and using ultrasonic dispersion for 15 min. The experiments of selectivity detection were conducted by immersing the samples in mixtures of M^{x+} aqueous solutions. Simultaneously, in order to determine of LOD for sensing Hg^{2+} ions,

a series of Hg^{2+} solutions of different concentrations were prepared and the emission of the samples upon addition were measured.

Table S1. Crystal data and structure refinement of TMU-46

Empirical formula	**C_{46} H_{30} Cu_2 N_4 $O_{12,2}$(C_3 H_7 N O),0.65(C_3 H_7 N O),0.6(C_3 H_7 N O)**
Chemical formula weight	**1206.99**
Crystal system	**monoclinic**
Space group	**P 21/n**
Temperature (K)	**190(2)**
Wavelength,MoKα (Å)	**0.71075**
a (Å)	**16.1139(12)**
b(Å)	**15.7868(11)**
c (Å)	**24.2833(18)**
α(°)	**90**
β(°)	**91.623(5)**
γ (°)	**90**
Cell volume (Å^3)	**6174.88**
Z	**4**
Z'	**0**
wR_factor_gt	**0.3461**
goodness_of_fit_ref (GOF)	**1.268**
R_factor_gt	**0.1381**
crystal_size_max **crystal_size_mid** **crystal_size_min**	**0.250** **0.150** **0.050**
crystal_F_000	**2496**
reflns_number_total	**10959**
crystal_colour	**green**

crystal_description	**platelet**

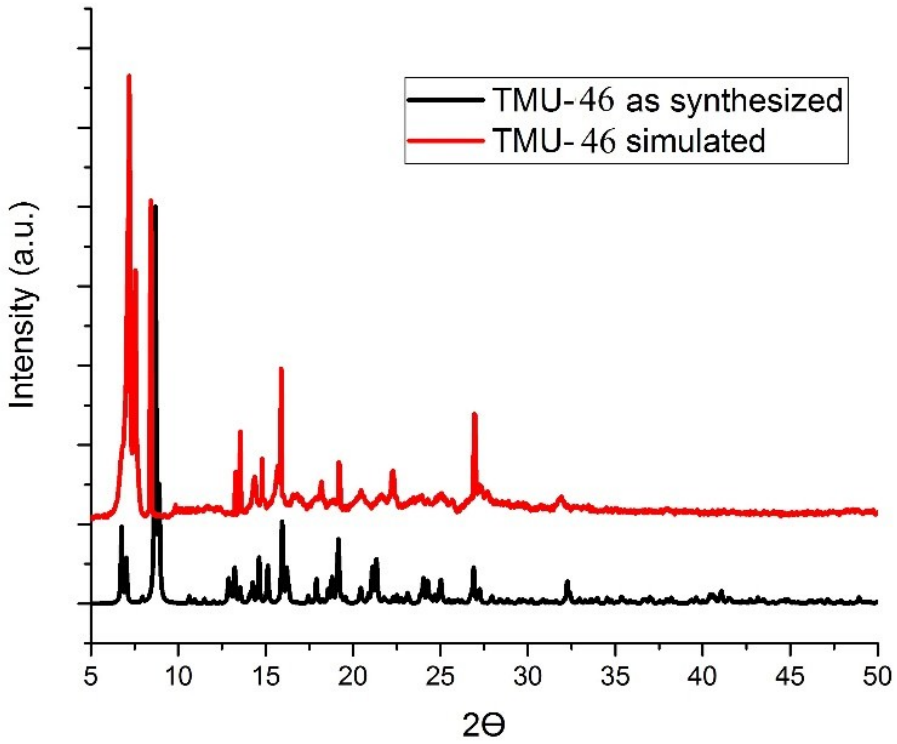

Fig.S1: PXRD spectra (black) of the synthesized TMU-46 and the simulated PXRD curve (red)

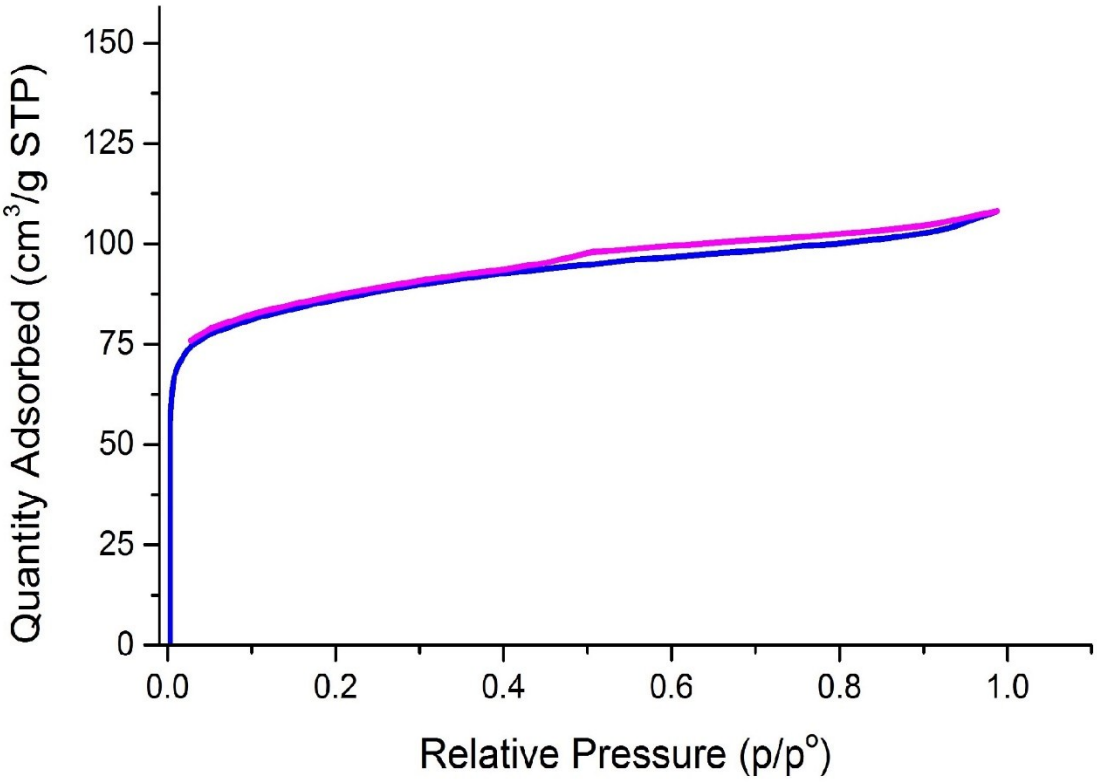

Fig.S2: Nitrogen adsorption-desorption isotherms at 77 K. TMU-48S after Hg2+ adsorption

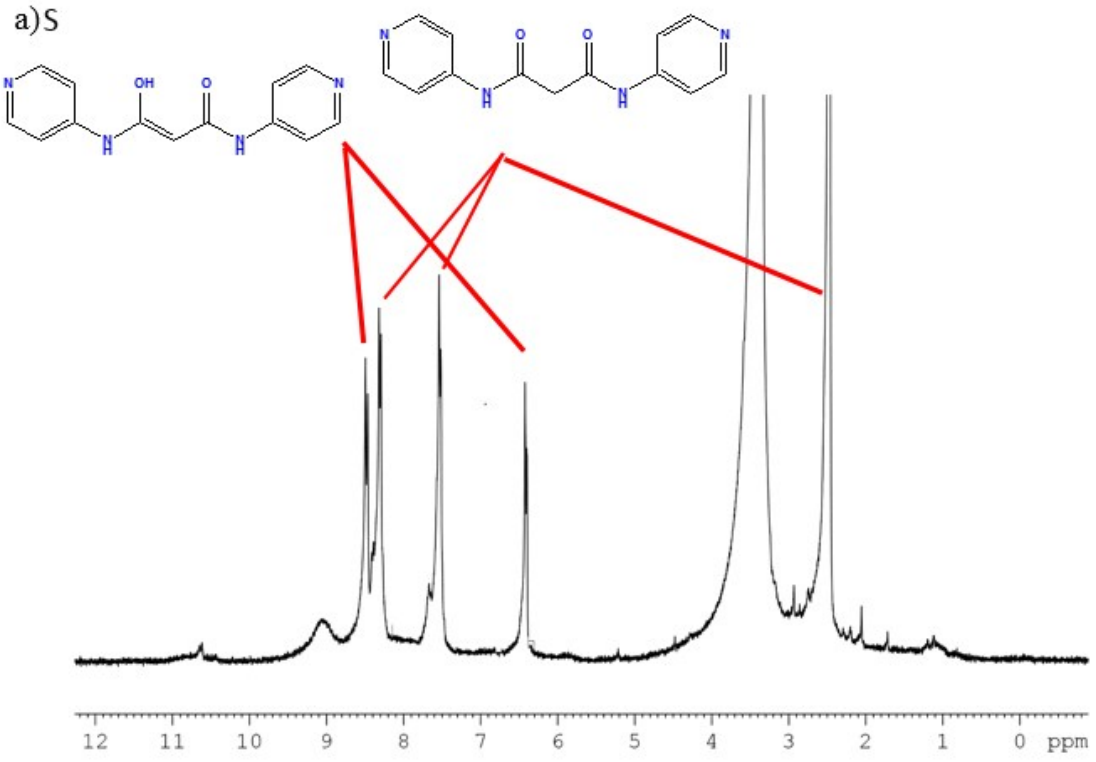

b) bpfb

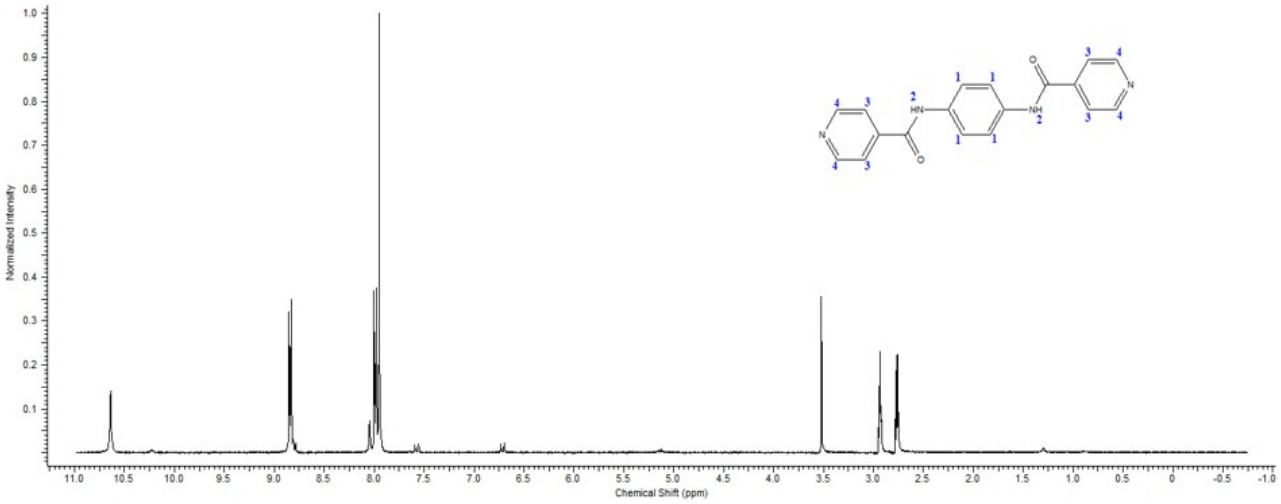

c) bpta

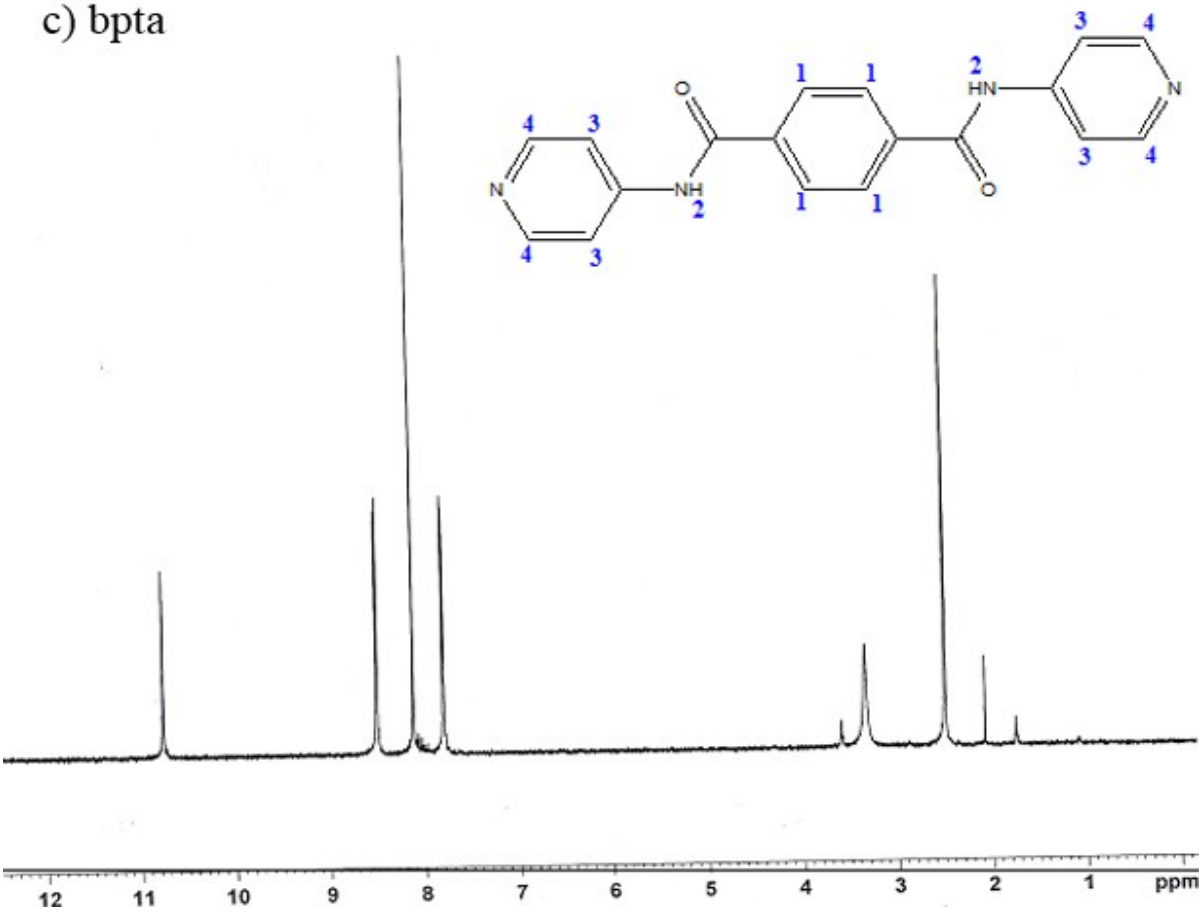

d) TMU-46S

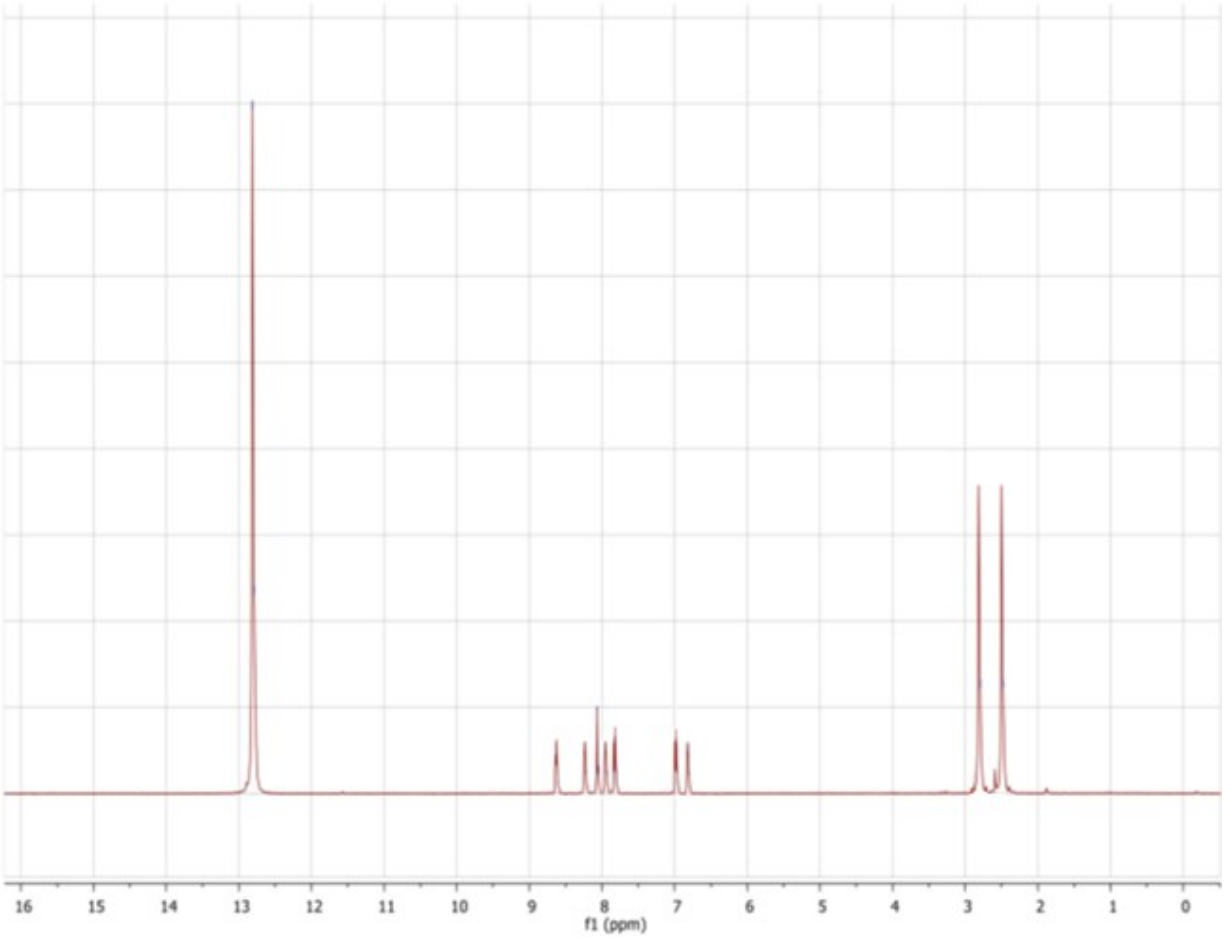

d´) TMU-46S

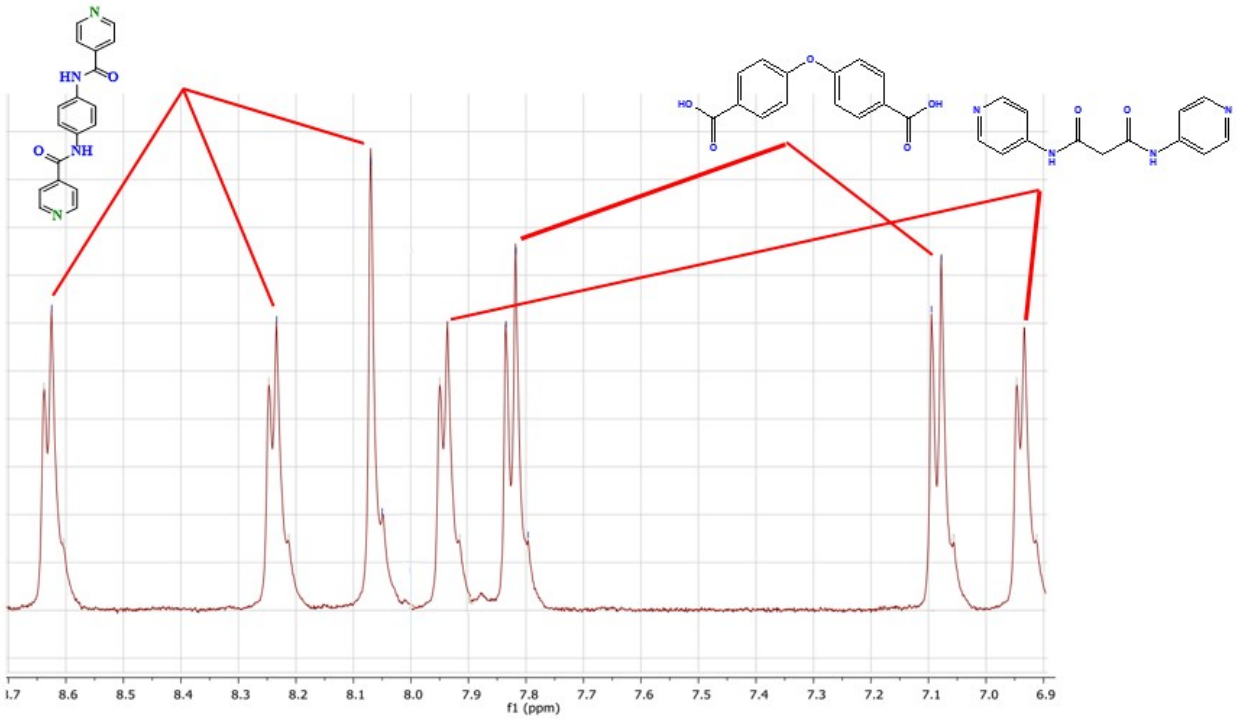

e)TMU-47S

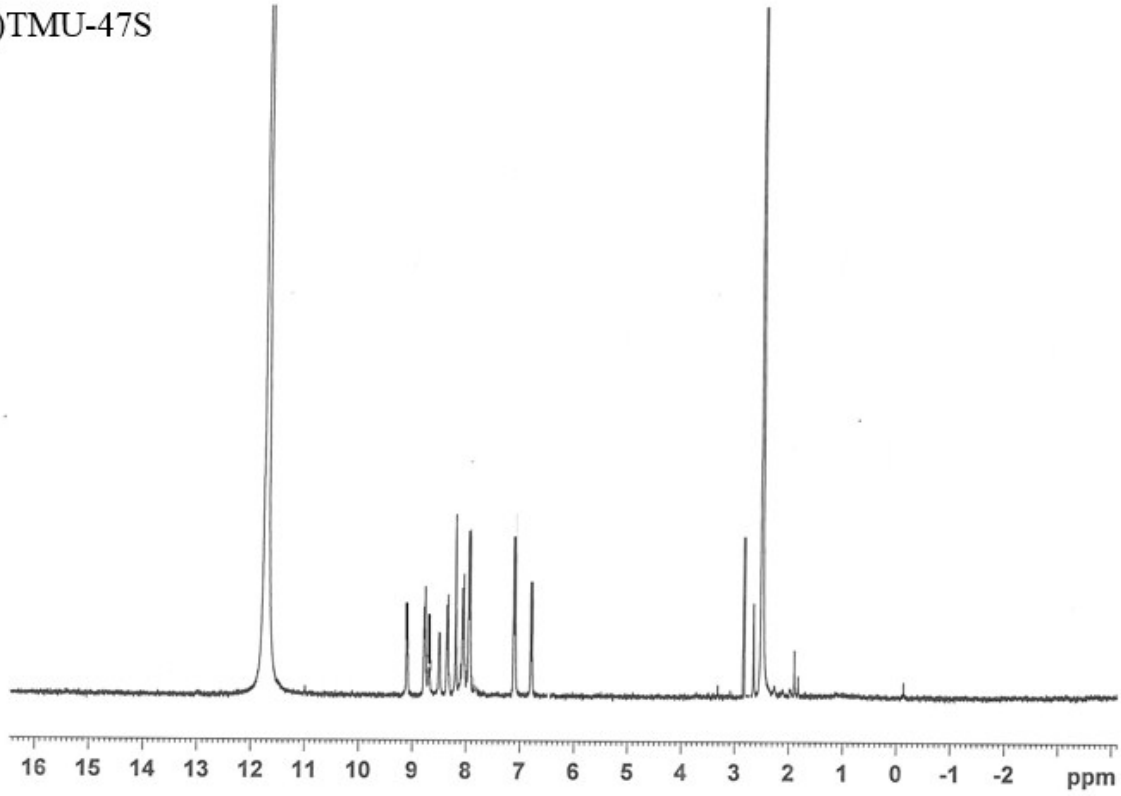

e´)TMU-47S

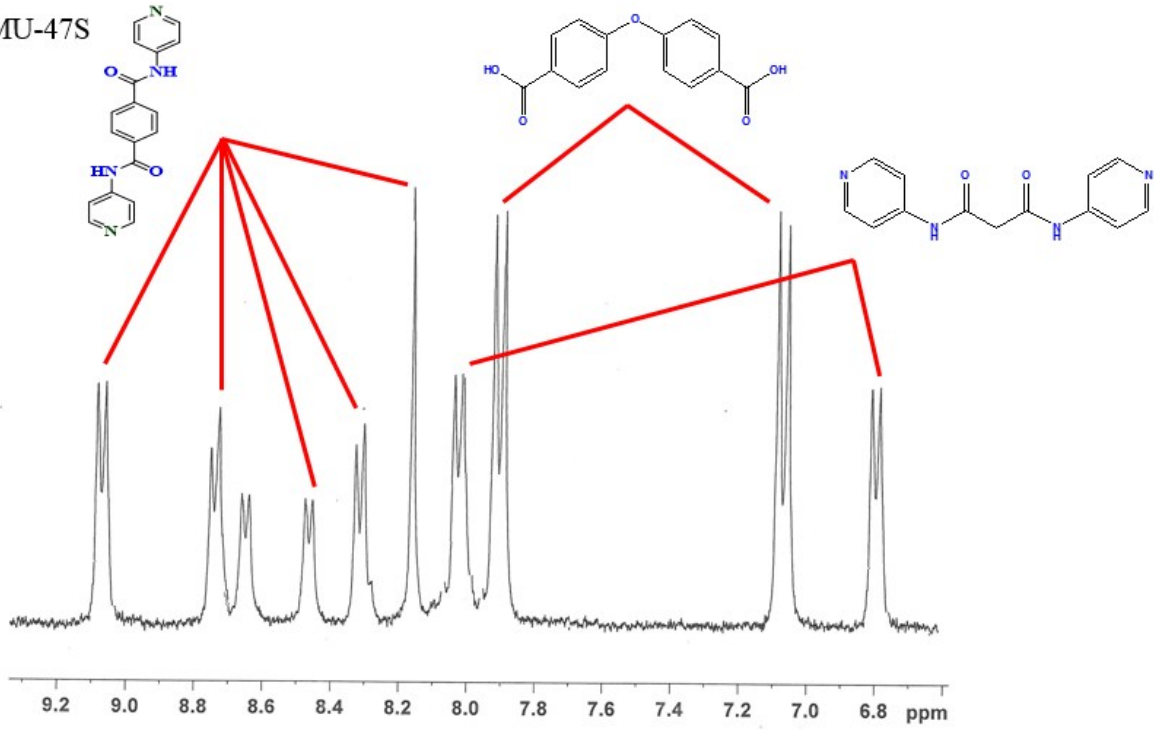

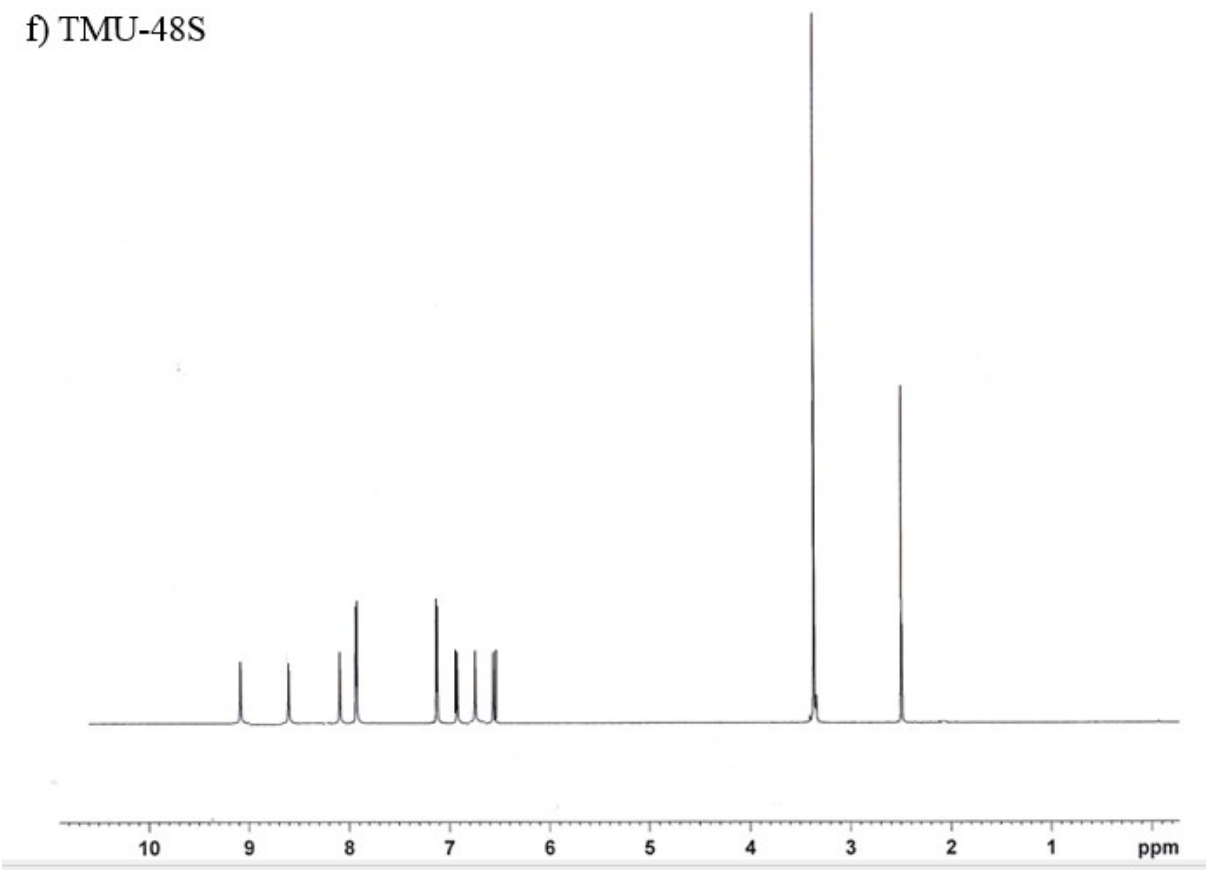

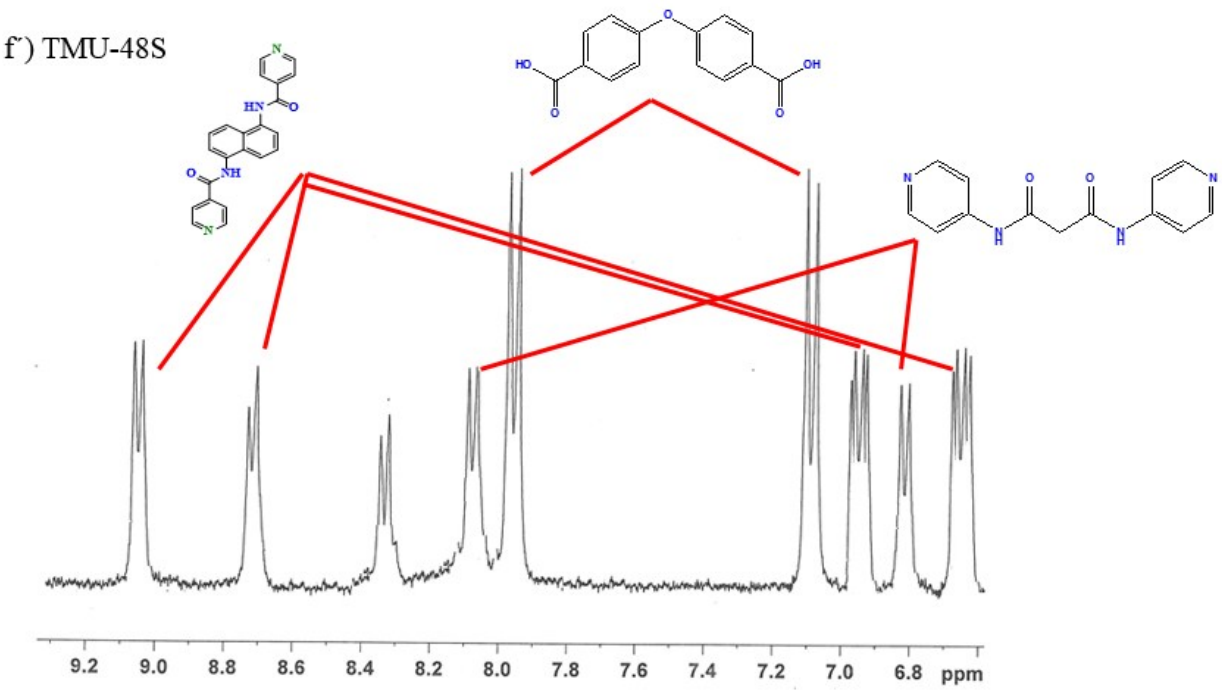

Fig.S3: NMR of compound TMU-46S, 47S and 48S (a: S ligand, b: bpta, c: bpfb d: NMR spectrum of TMU-46 d´: expanded spectrum of TMU-46 e: NMR spectrum of TMU-47 e´: expanded spectrum of TMU-47 f: NMR spectrum of TMU-489 f´: expanded spectrum of TMU-48).

Table S2. The area under the curve in NMR spectra

Sample	The area under the curve in NMR spectra						
	6.95 ppm	7.07 ppm	7.82 ppm	7.95 ppm	8.07 ppm	8.25 ppm	8.62 ppm
TMU-46S	1.47	1.71	1.68	1.5	1	1.54	1.58
	^3J:7.5 Hz	^3J:8 Hz	^3J:8 Hz	^3J:7.5 Hz	-	^3J:8.3Hz	^3J:8.3Hz

Sample	The area under the curve in NMR spectra									
	8.65 ppm	6.8 ppm	7.1 ppm	7.9 ppm	8.05 ppm	8.3 ppm	8.5 ppm	8.65 ppm	8.75 ppm	9.05 ppm
TMU-47S	1.87	3.14	3.12	2	1.38	1.53	1	1.05	1.61	1.92
	^3J:7.2 Hz	^3J:7.3 Hz	^3J:7.3 Hz	^3J:7.2 Hz	-	^3J:7.5 Hz	^3J:7.2 Hz	^3J:7.2 Hz	^3J:7.5 Hz	^3J:7.5 Hz

Sample	The area under the curve in NMR spectra								
	6.65 ppm	6.8 ppm	6.95 ppm	7.1 ppm	7.95 ppm	8.1 ppm	8.35 ppm	8.7 ppm	9.05 ppm
TMU-48S	1.73	1.44	1.75	2.46	2.48	1.48	0.98	1.43	1.82
	^3J:9.4Hz ^4J:3.8 Hz	^3J:7.5 Hz	^3J:9.4Hz ^4J:3.8 Hz	^3J:7.3 Hz	^3J:7.3 Hz	^3J:7.5 Hz	^3J:7.5 Hz	^3J:7.3 Hz	^3J:7.3 Hz

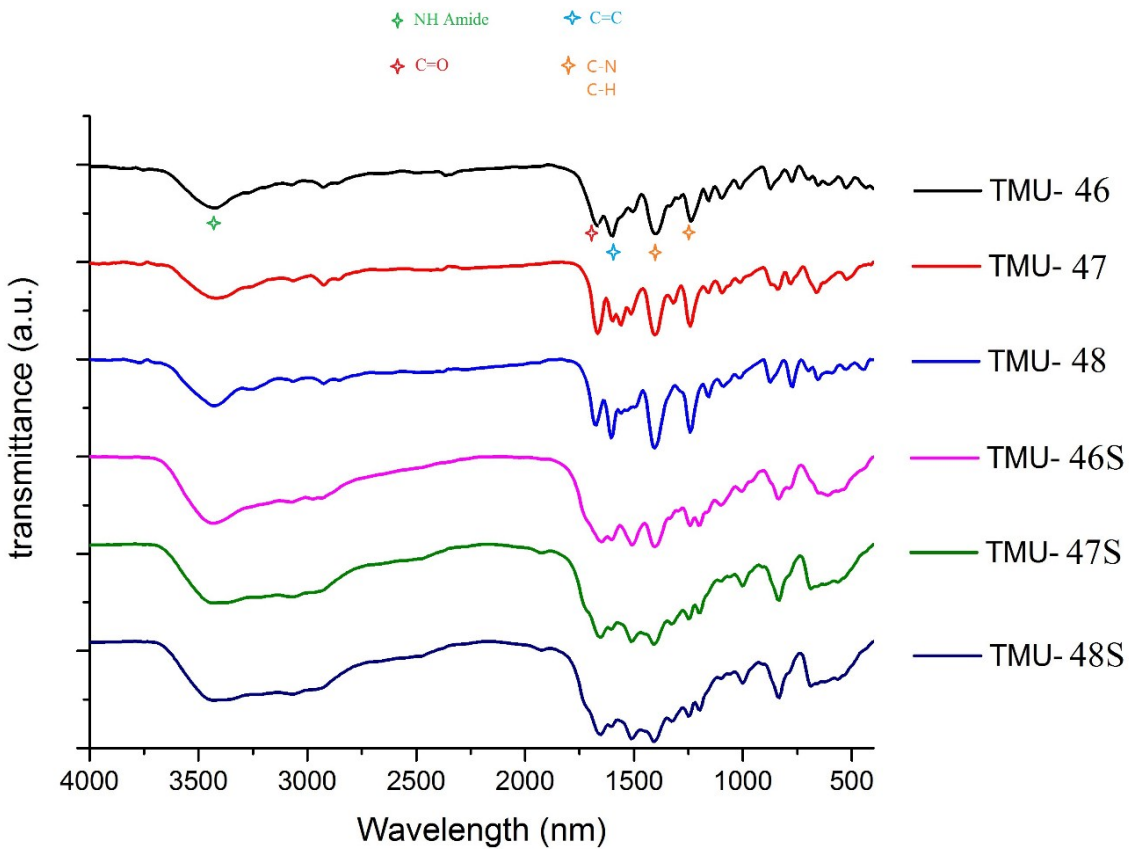

Fig. S4: IR spectroscopy of the TMU-46 (black), TMU-47 (red) and TMU-48 (blue), The IR spectroscopy of TMU-46S (pink), TMU-47S (green) and

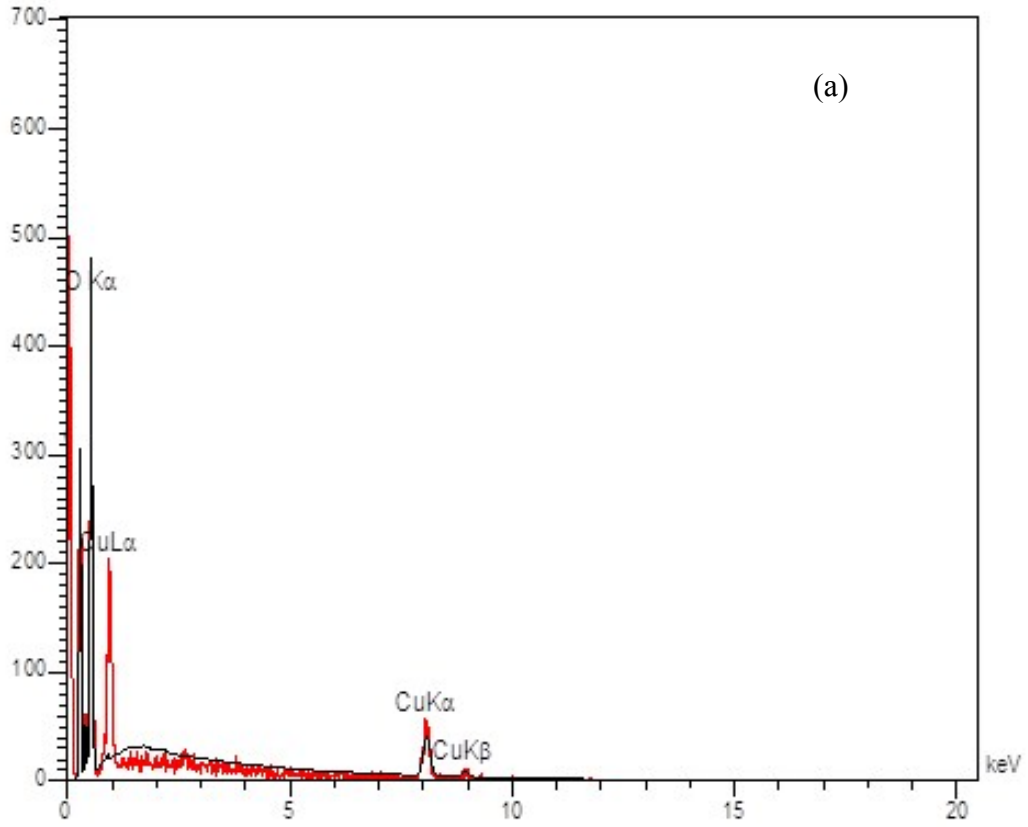

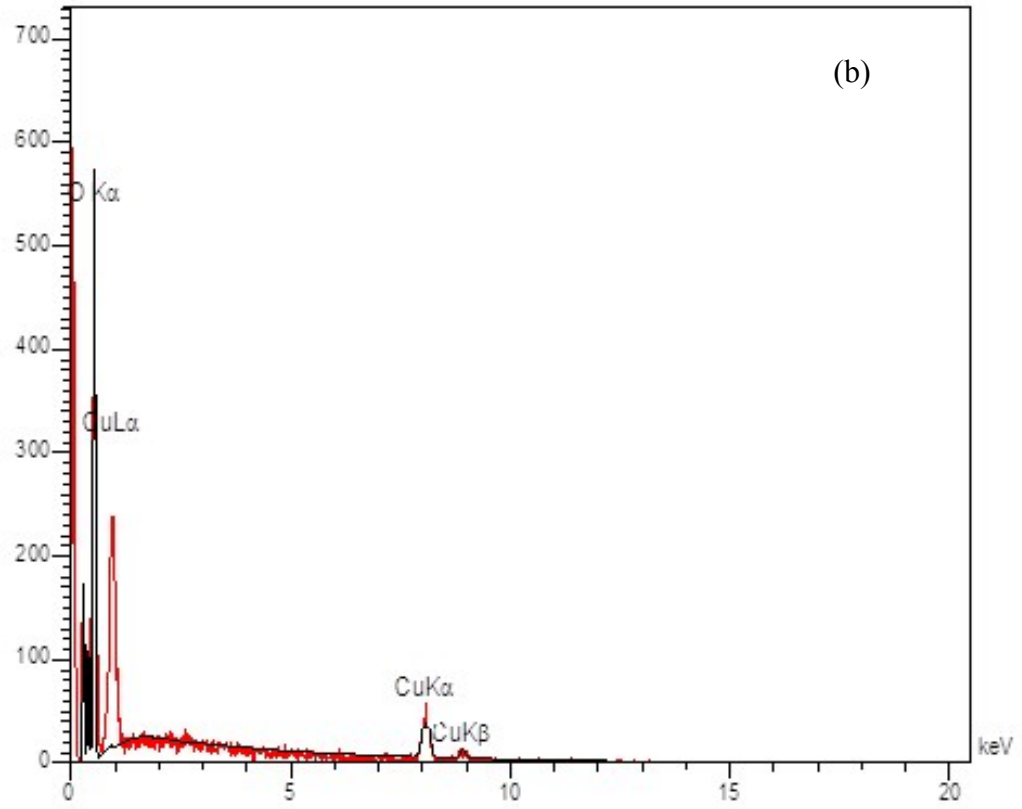
(b)
700
600
500
400
300
200
100
0
O Kα
CuLα
CuKα
CuKβ
keV
0
5
10
15
20

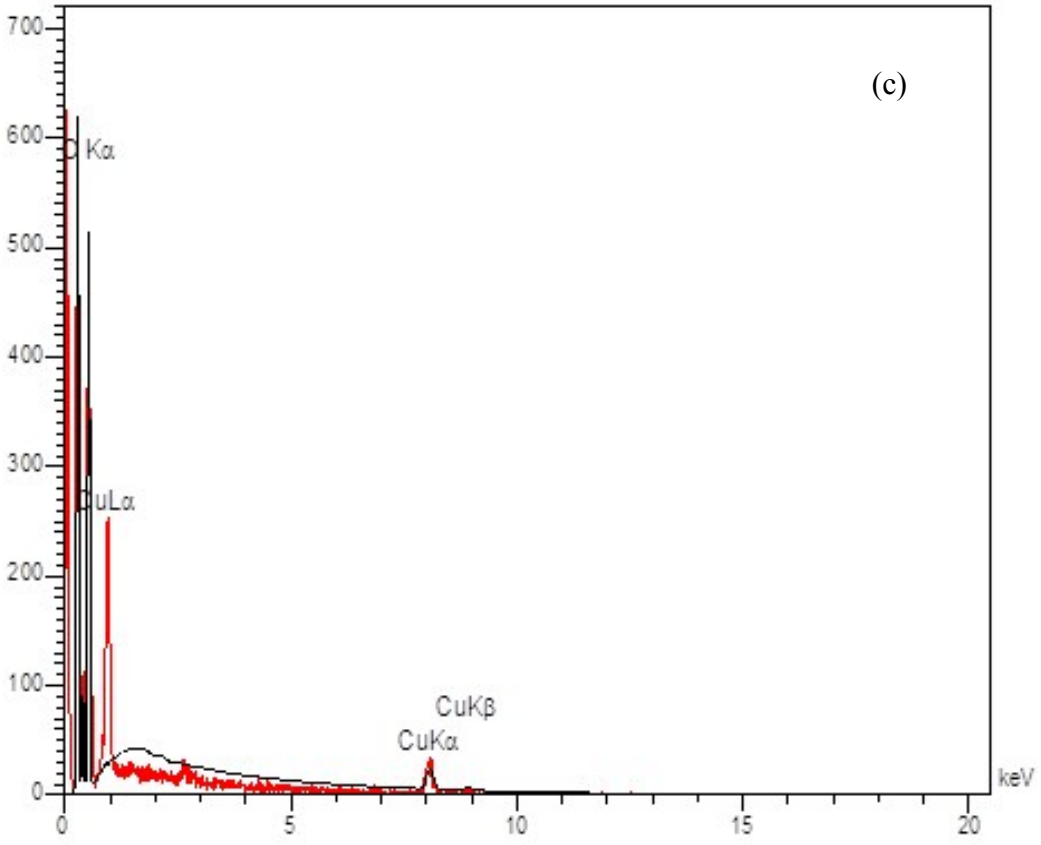
(c)
700
600
500
400
300
200
100
0
O Kα
CuLα
CuKβ
CuKα
keV
0
5
10
15
20

(d)

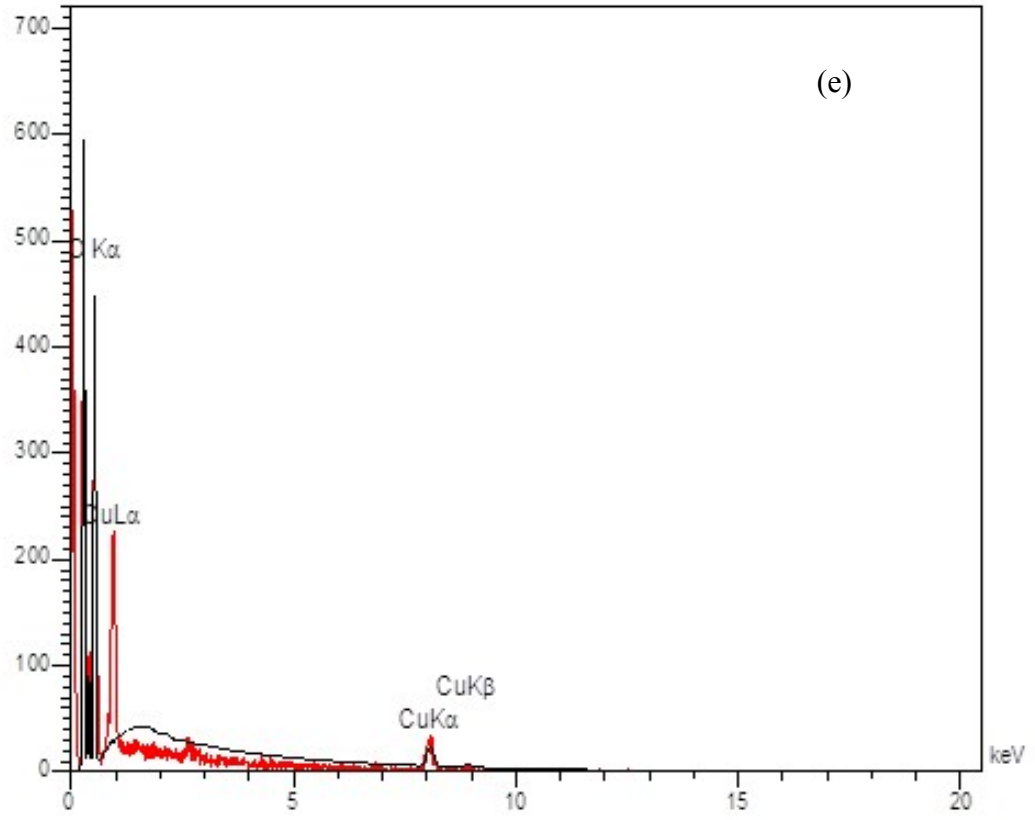
(e)
700
600
500
400
300
200
100
0
O Kα
CuLα
CuKβ
CuKα
keV
0
5
10
15
20

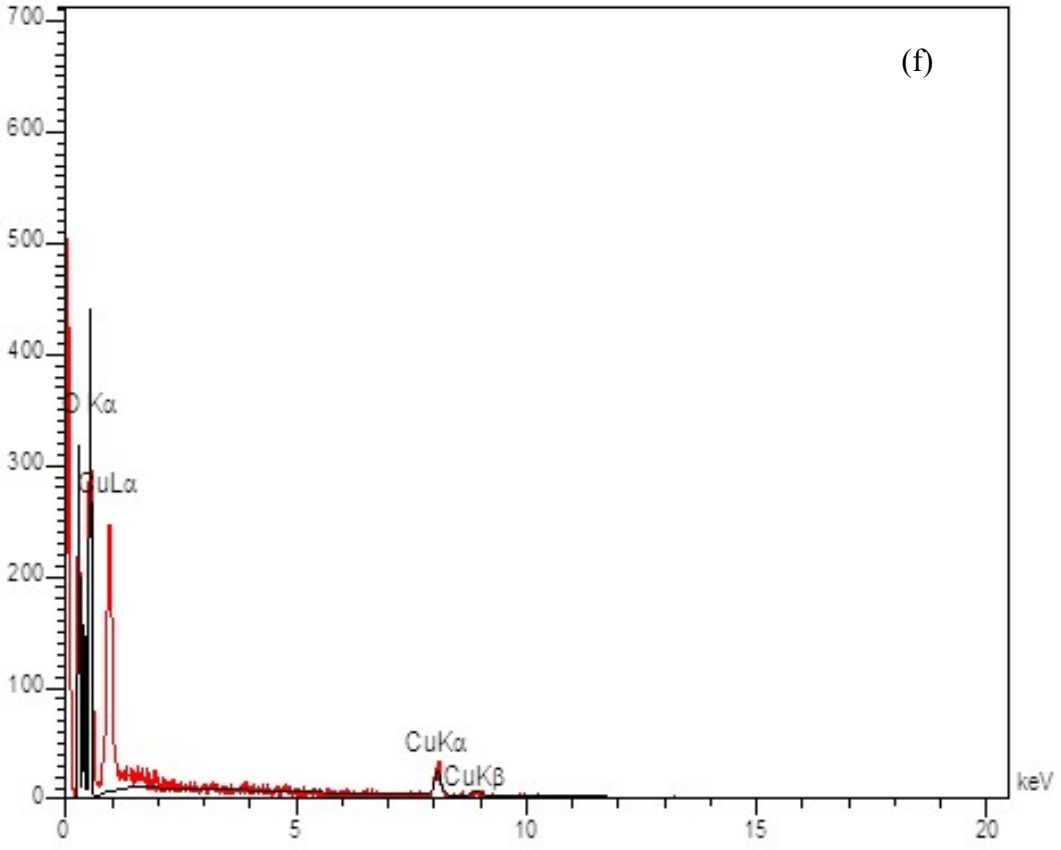
(f)
700
600
500
400
300
200
100
0
O Kα
CuLα
CuKα
CuKβ
keV
0
5
10
15
20

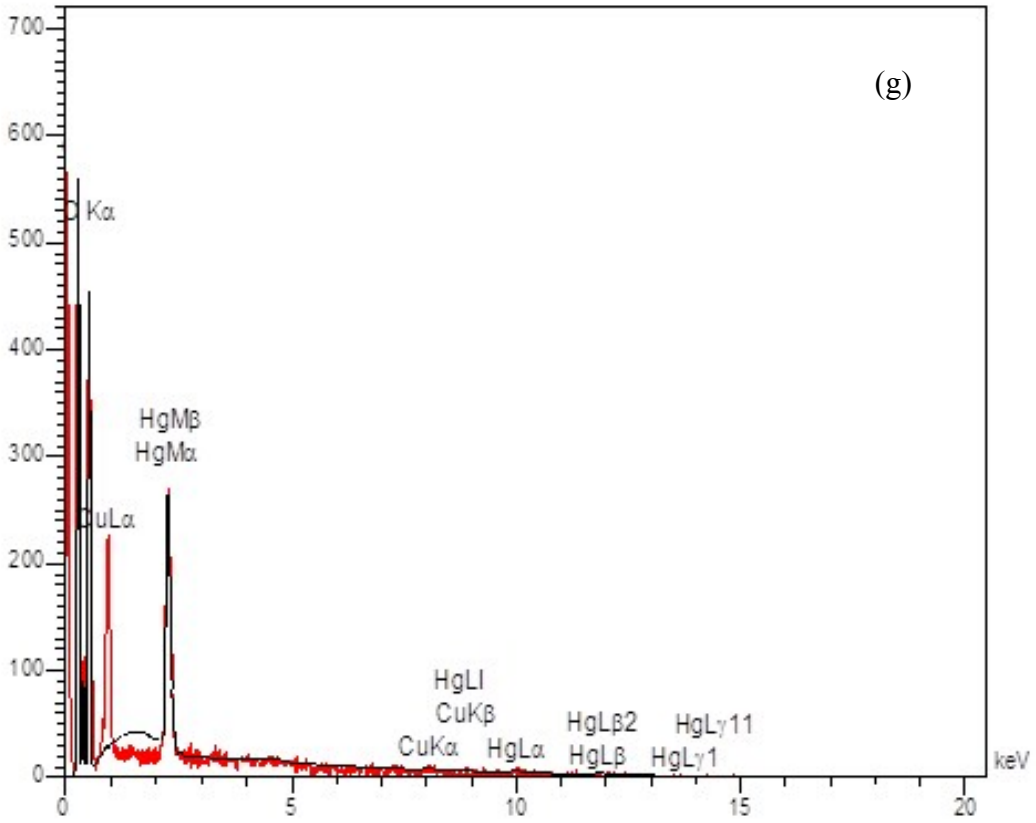

Fig. S5: Elemental analysis from EDS data : a)TMU-46, b)TMU-46S, c)TMU-47, d)TMU-47S, e)TMU-48, f)TMU-48S, g)TMU-48S after Hg^{2+} adsorbtion

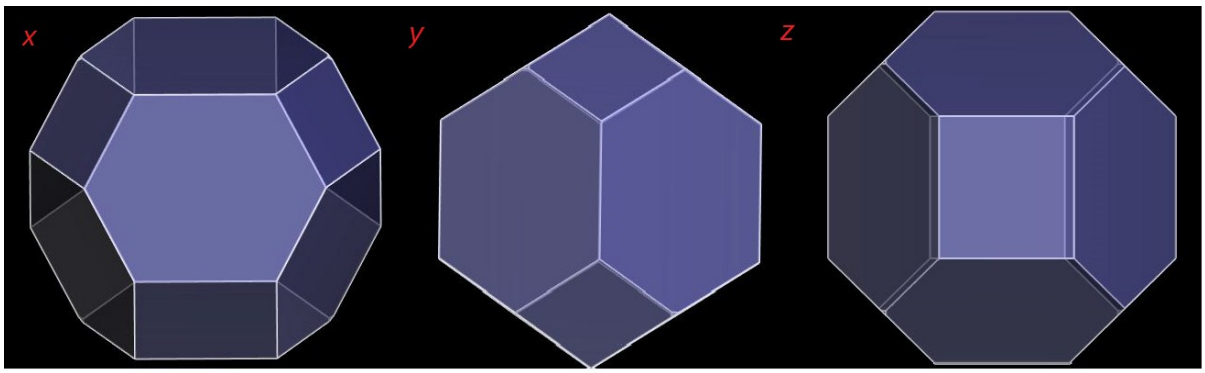

Fig. S6: Predicted morphology of TMU-46 in DMF by BFDH method

Fluorescence Measurements

The Fluorescence properties of TMU-46, TMU-47 and TMU-47 and their daughter compounds were measured in water containing MOFs using a PerkinElmer-LS55 Fluorescence Spectrometer at room temperature. In a typical procedure, 3 mg of an activated MOF was grinded down, and then immersed in different analyte solutions (3 ml) and after 1 hours was tested in the emission mode. For fluorescence measurement in the presence of metal cations.

Stern-Volmer Plots

According to the Stern-Volmer equation, $(I_0/I)= K_{SV}$ [A] + 1,Where here, I_0 is the initial fluorescence intensity of soaked MOF sample in toluene, I is the fluorescence intensity in the presence of analyte, [A] is the molar concentration of analyte, and K_{SV} is the Stern-Volmer constant (M^{-1}). For the quenching constant extraction, emission intensity of MOFs was recorded by suspending them into different concentrations of analyte solutions in water, upon the same manner described in Fluorescence measurement section.

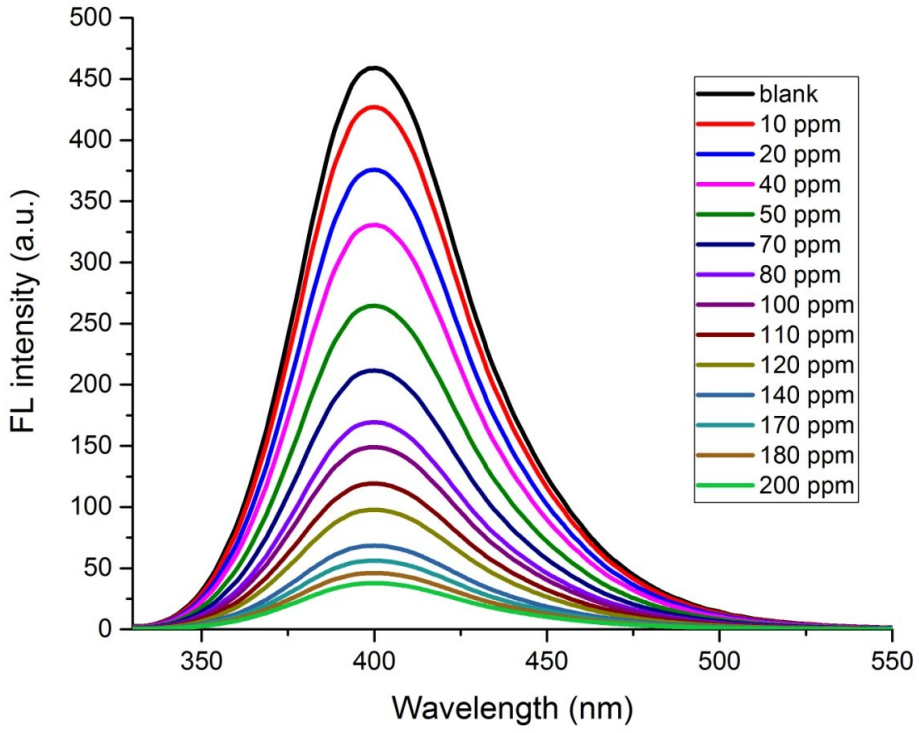

Figure **S7**. Fluorescence emission spectra of **TMU-46** dispersed in water solution at different concentrations of $\mathbf{Hg^{2+}}$, excited at 310 nm.

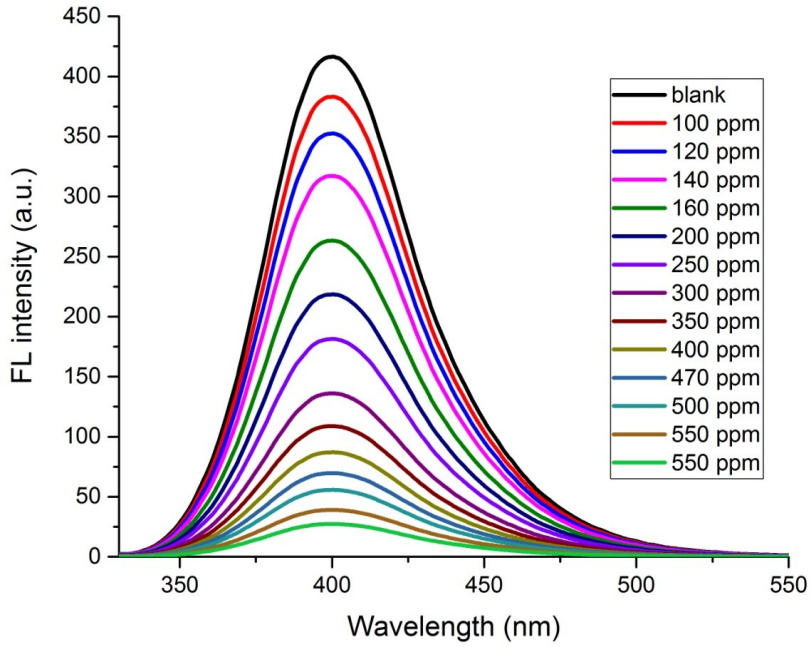

Figure **S8**. Fluorescence emission spectra of **TMU-46** dispersed in water solution at different concentrations of $\mathbf{Pb^{2+}}$, excited at 310 nm.

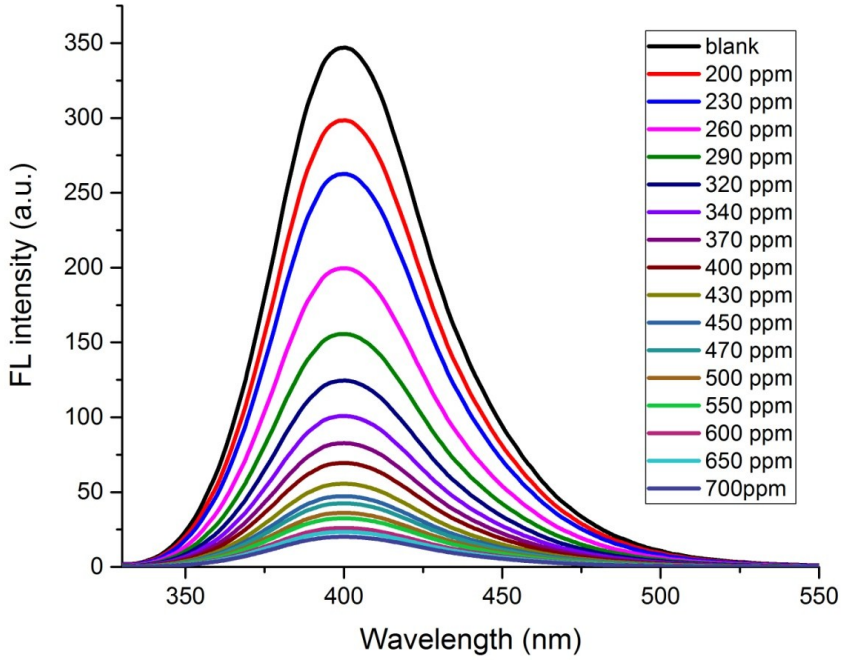

Figure **S9**. Fluorescence emission spectra of **TMU-46** dispersed in water solution at different concentrations of $\mathbf{Ag^{+}}$, excited at 310 nm.

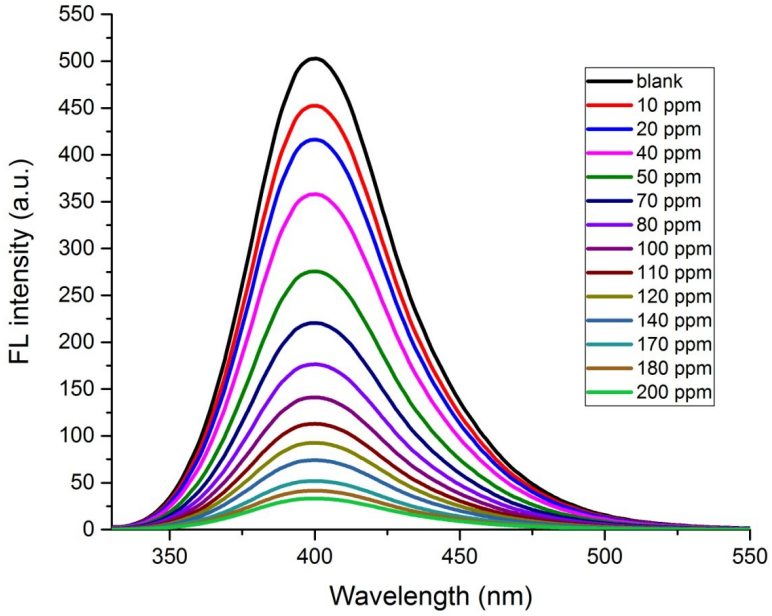

Figure **S10**. Fluorescence emission spectra of **TMU-47** dispersed in water solution at different concentrations of $\mathbf{Hg^{2+}}$, excited at 310 nm.

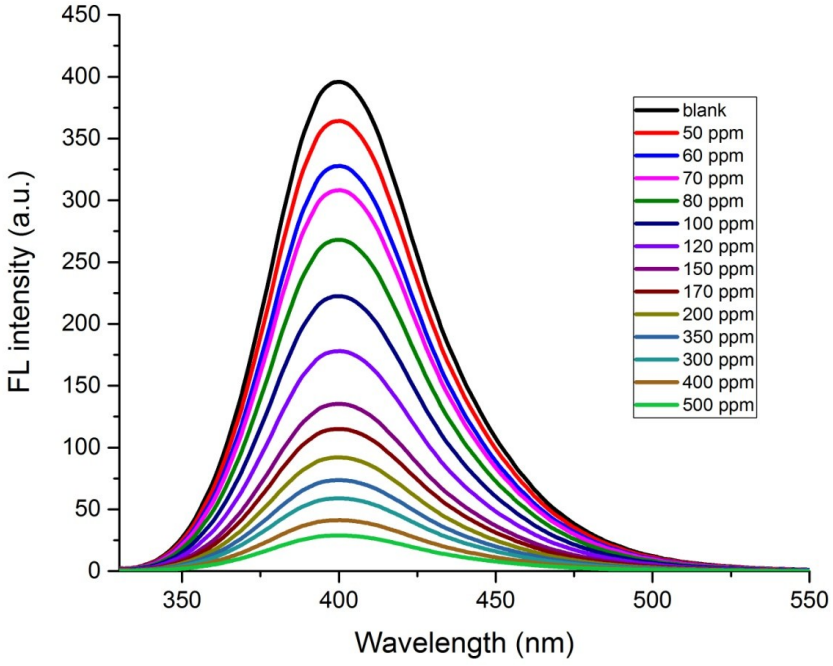

Figure **S11**. Fluorescence emission spectra of **TMU-47** dispersed in water solution at different concentrations of $\mathbf{Pb^{2+}}$, excited at 310 nm.

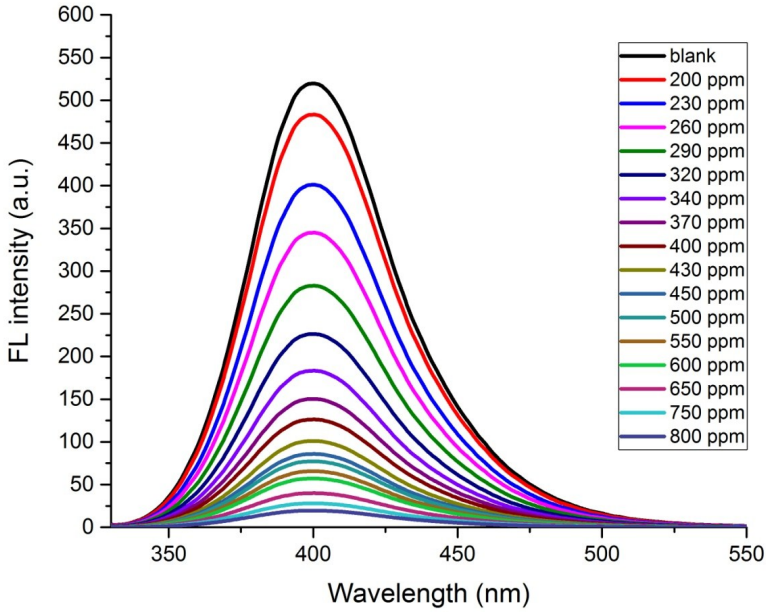

Figure **S12**. Fluorescence emission spectra of **TMU-47** dispersed in water solution at different concentrations of $\mathbf{Ag^{+}}$, excited at 310 nm.

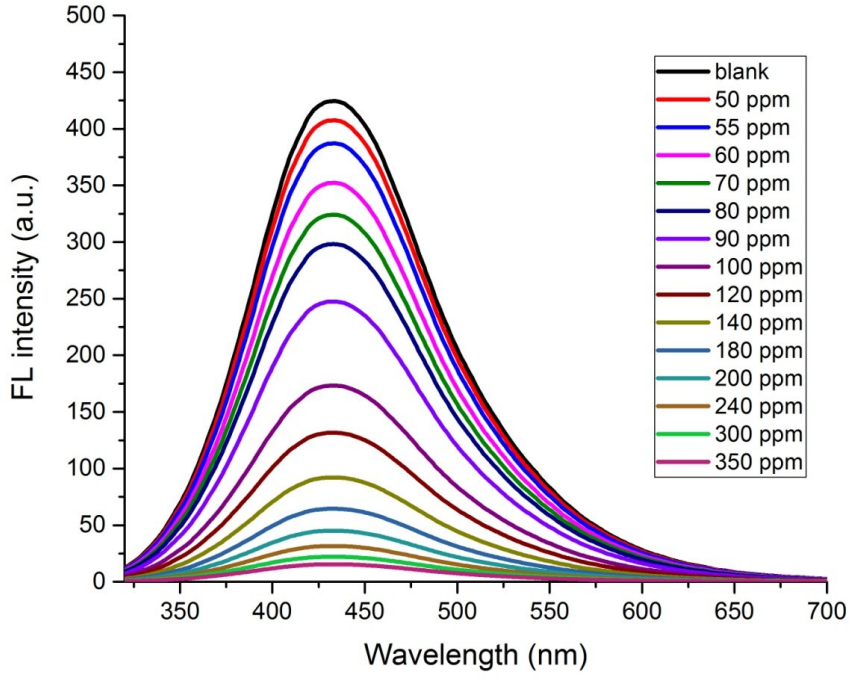

Figure **S13**. Fluorescence emission spectra of **TMU-48** dispersed in water solution at different concentrations of $\mathbf{Hg^{2+}}$, excited at 315 nm.

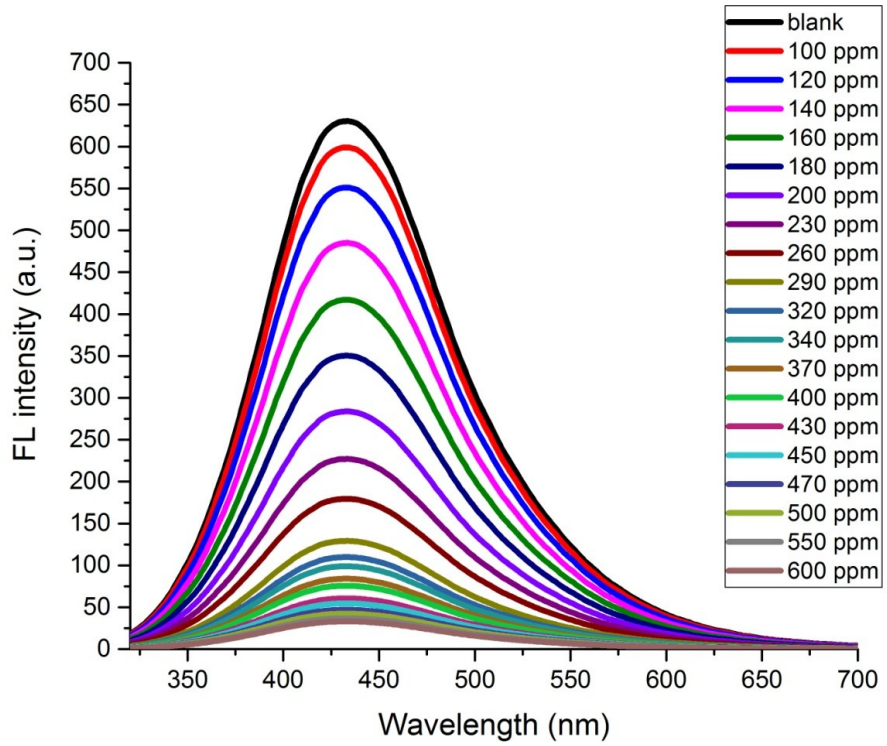

Figure **S14.** Fluorescence emission spectra of **TMU-48** dispersed in water solution at different concentrations of $\mathbf{Pb^{2+}}$, excited at 315nm.

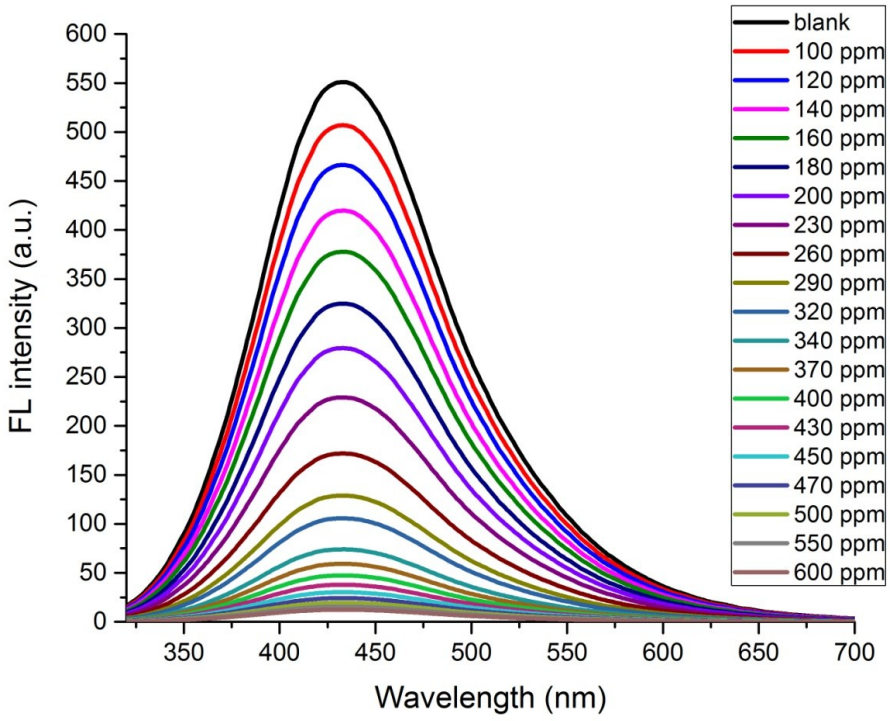

Figure **S15**. Fluorescence emission spectra of **TMU-48** dispersed in water solution at different concentrations of $\mathbf{Ag^{+}}$, excited at 315 nm.

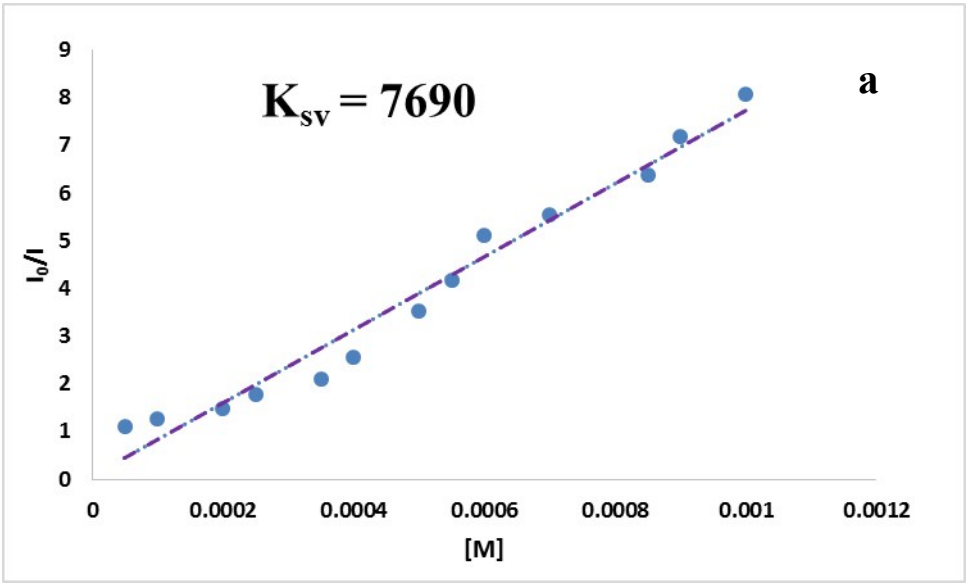
a
K_{sv} = 7690
I_0/I
[M]
0
1
2
3
4
5
6
7
8
9
0
0.0002
0.0004
0.0006
0.0008
0.001
0.0012

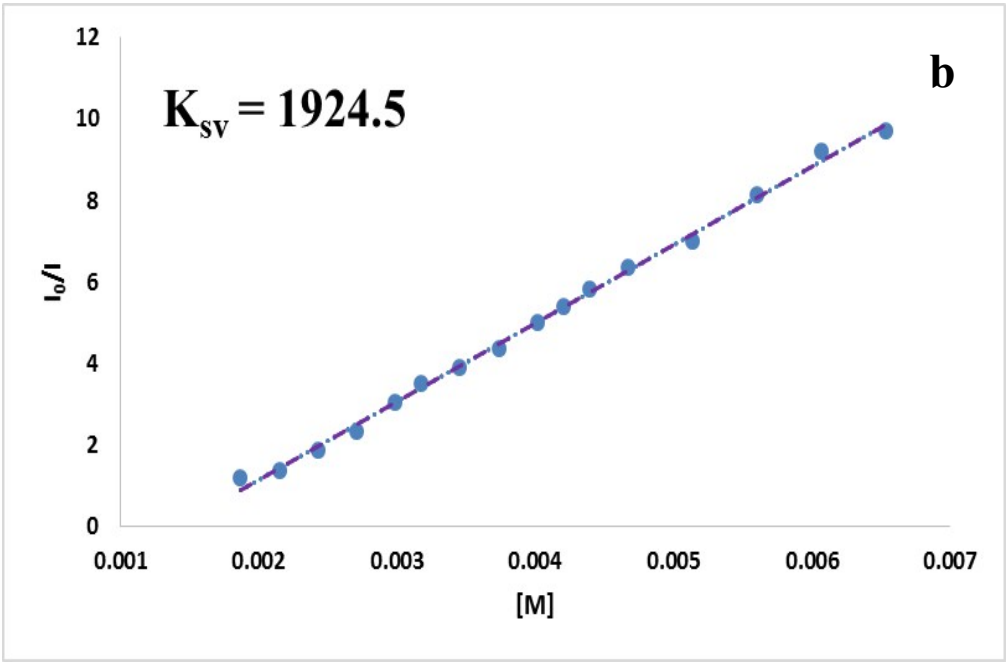
b
K_{sv} = 1924.5
I_0/I
[M]
0
2
4
6
8
10
12
0.001
0.002
0.003
0.004
0.005
0.006
0.007

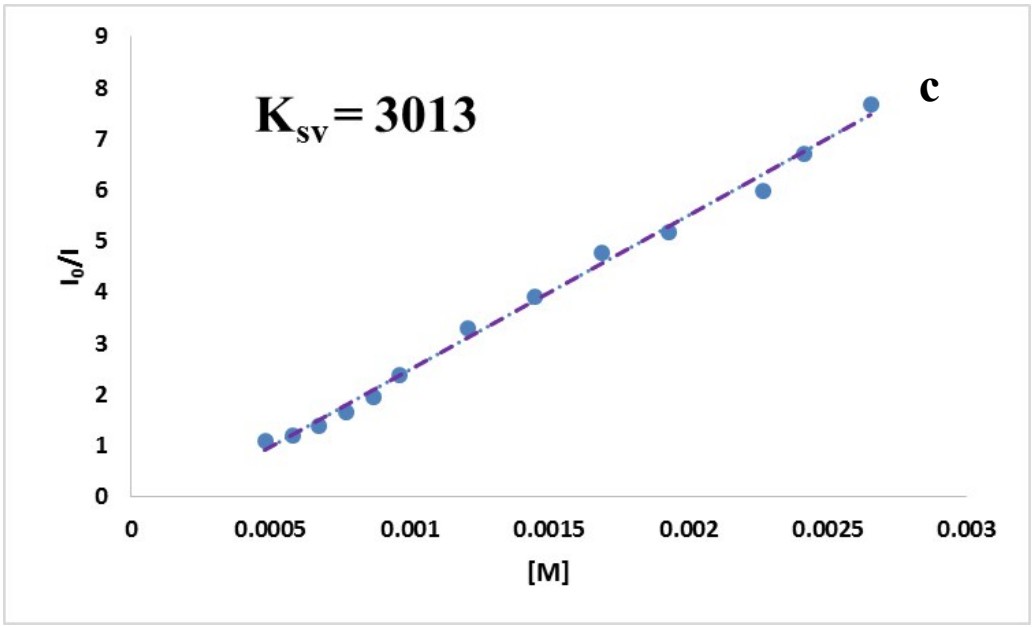

Figure **S16**. Stern–Volmer (SV) plots in the presence of 3 mg of **TMU-46** in different Hg^{2+} (a) Ag^{+} (b) pb^{2+} (c) concentrations ([Q]) in water.

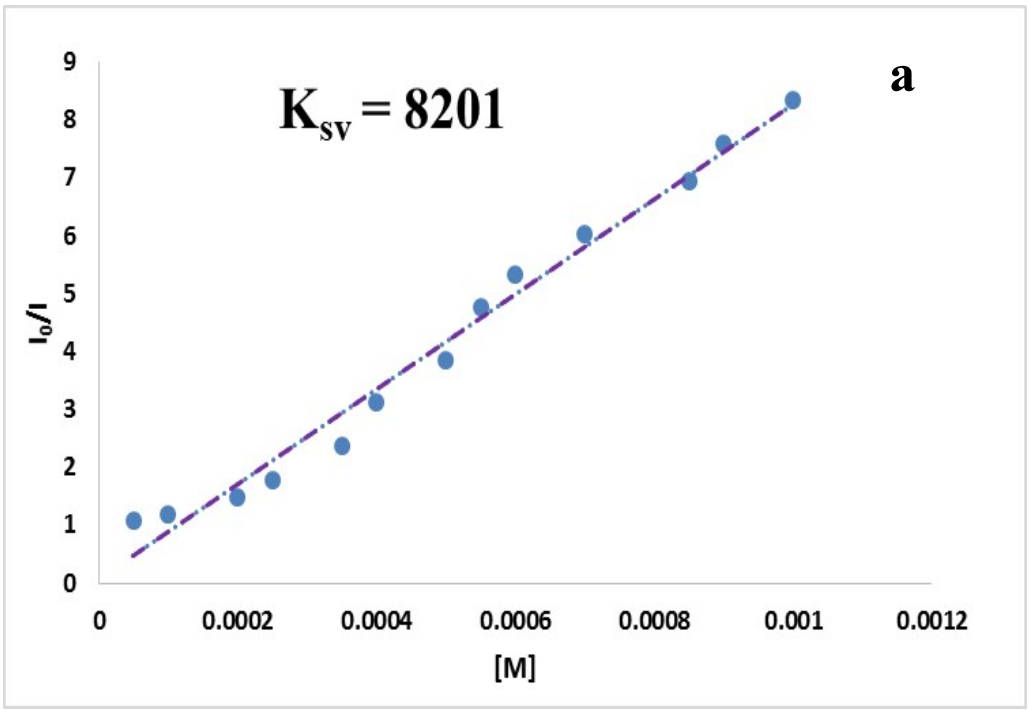

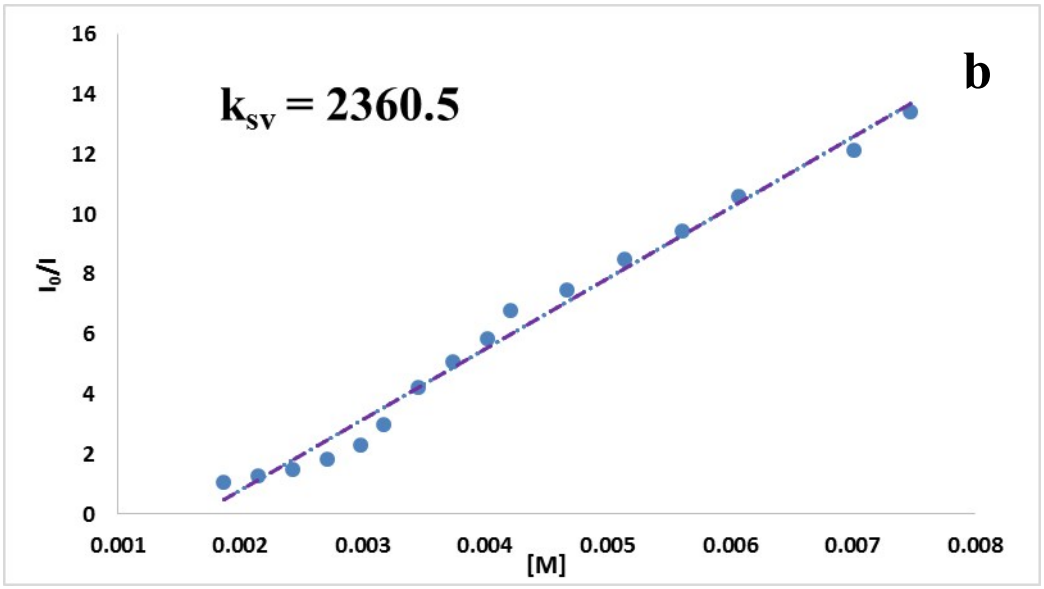

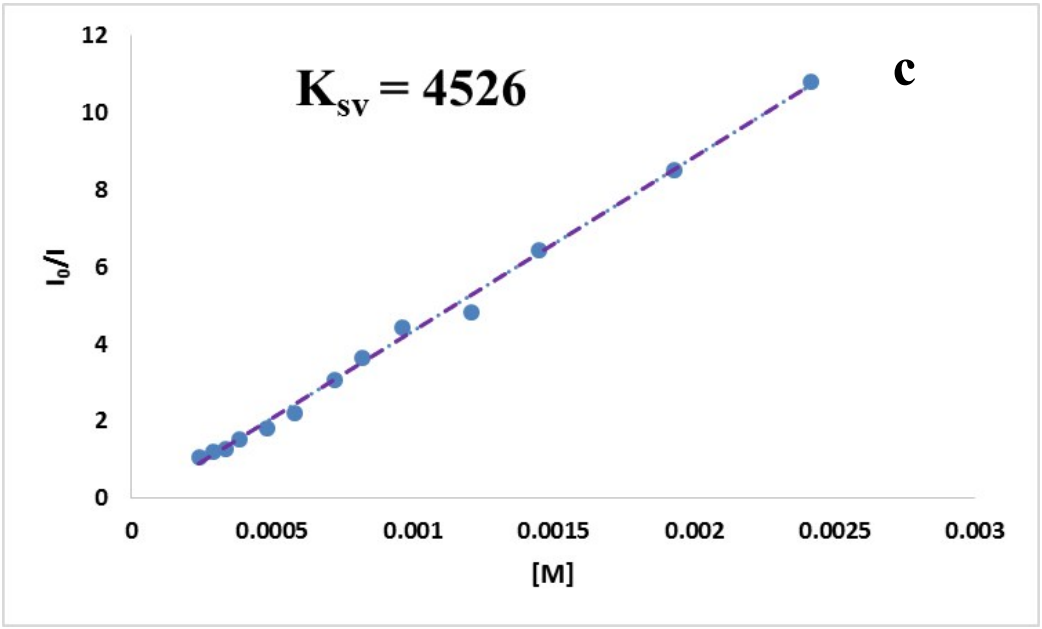

Figure **S17**. Stern–Volmer (SV) plots in the presence of 3 mg of **TMU-47** in different Hg^{2+} (a) Ag^{+} (b) pb^{2+} (c) concentrations ([Q]) in water.

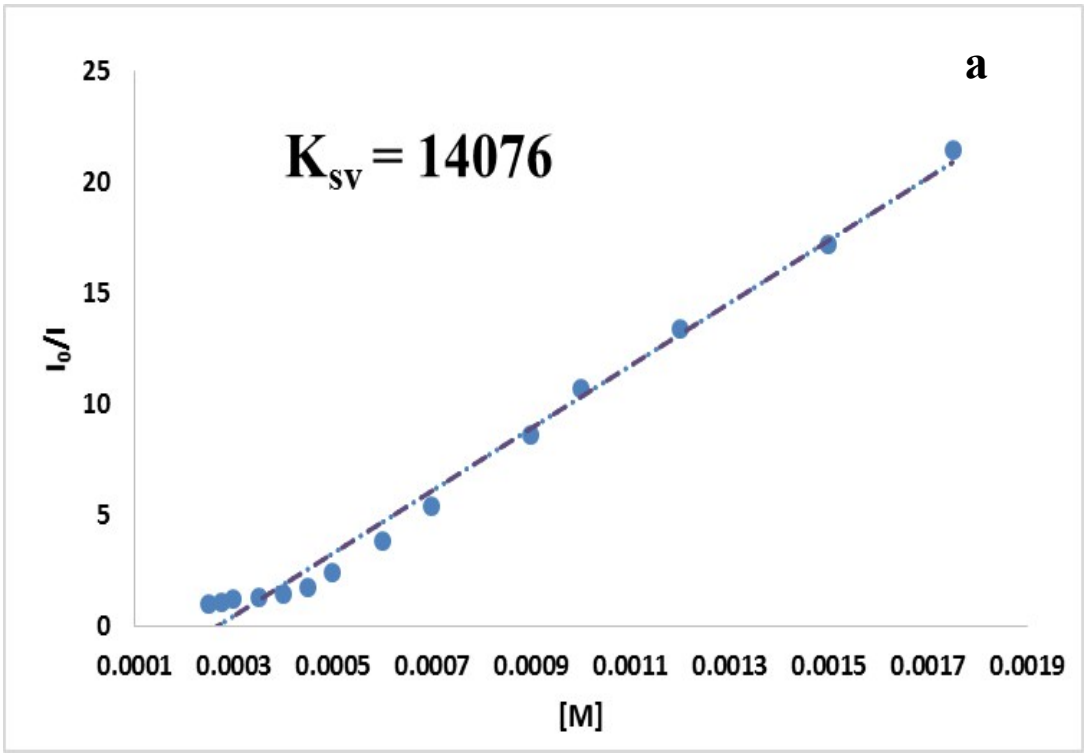
a
K_{sv} = 14076
I_0/I
25
20
15
10
5
0
0.0001
0.0003
0.0005
0.0007
0.0009
0.0011
0.0013
0.0015
0.0017
0.0019
[M]

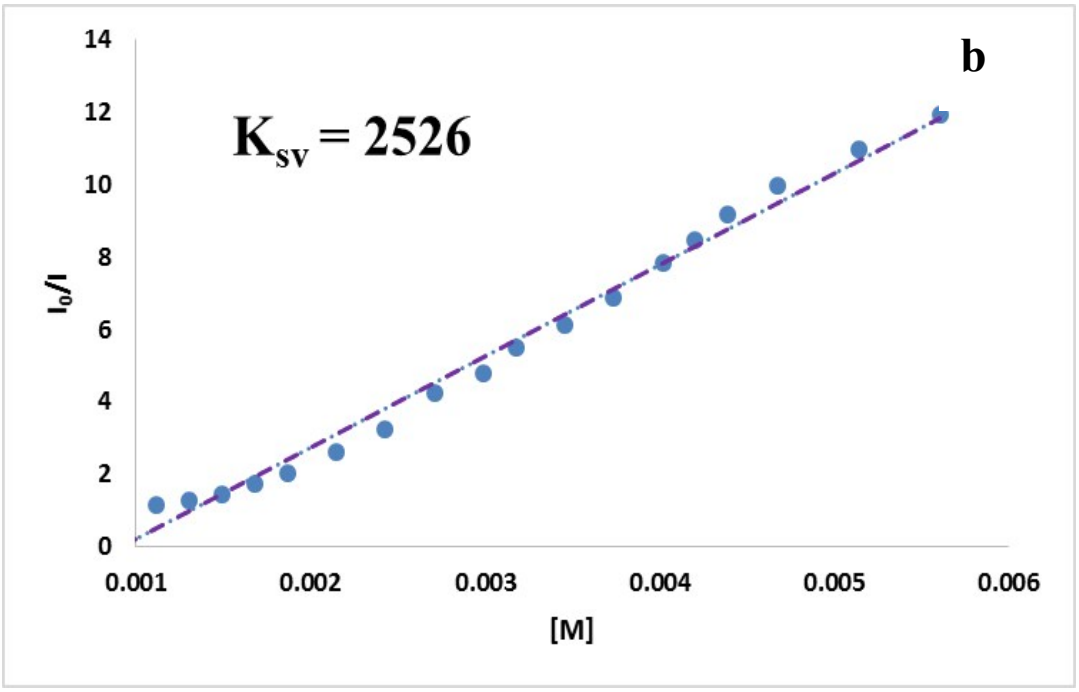
b
K_{sv} = 2526
I_0/I
14
12
10
8
6
4
2
0
0.001
0.002
0.003
0.004
0.005
0.006
[M]

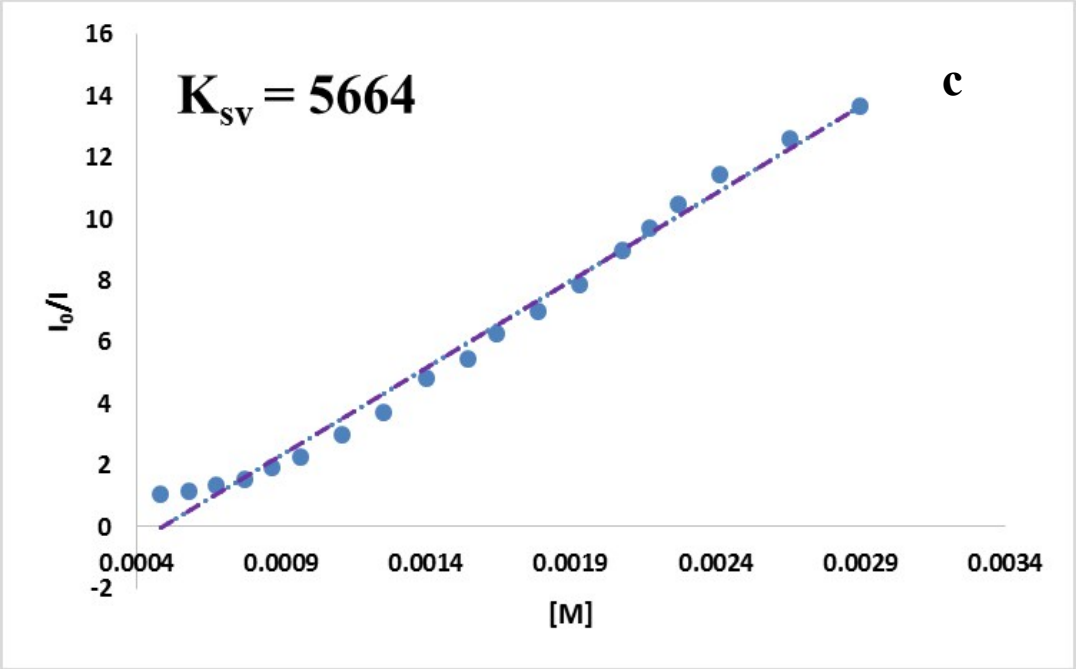

Figure **S18**. Stern–Volmer (SV) plots in the presence of 3 mg of **TMU-48** in different $\mathbf{Hg^{2+}}$ (a) $\mathbf{Ag^{+}}$ (b) $\mathbf{pb^{2+}}$ (c) concentrations ([Q]) in water.

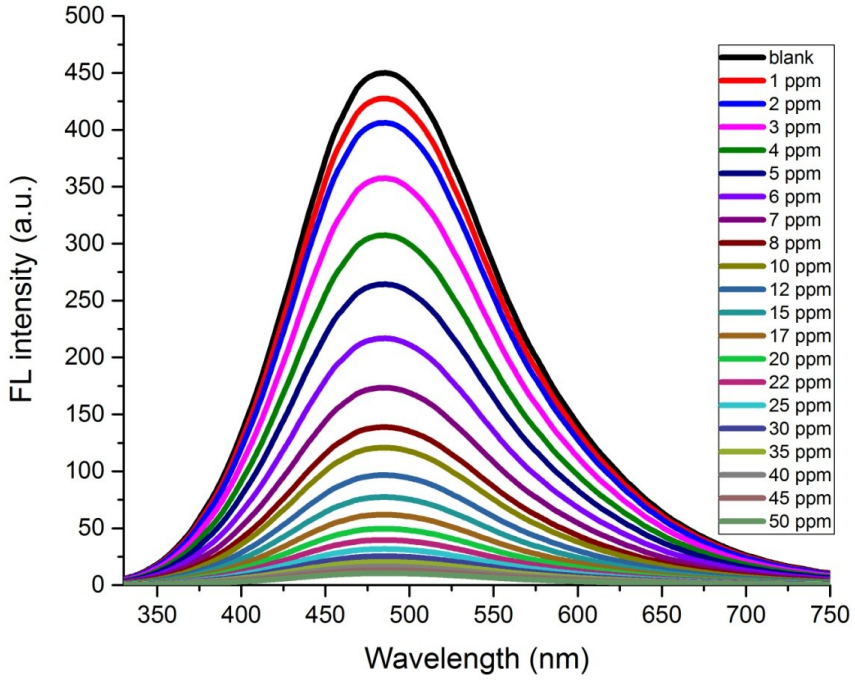

Figure **S19**. Fluorescence emission spectra of **TMU-46S** dispersed in water solution at different concentrations of $\mathbf{Hg^{2+}}$, excited at 320 nm.

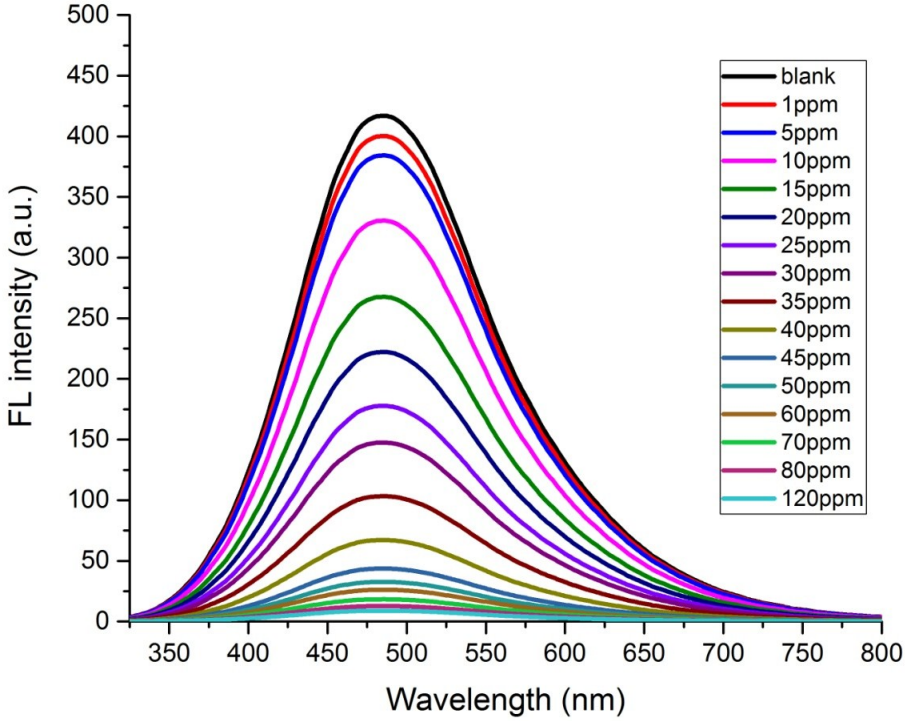

Figure **S20**. Fluorescence emission spectra of **TMU-46S** dispersed in water solution at different concentrations of $\mathbf{Ag^{+}}$, excited at 320 nm.

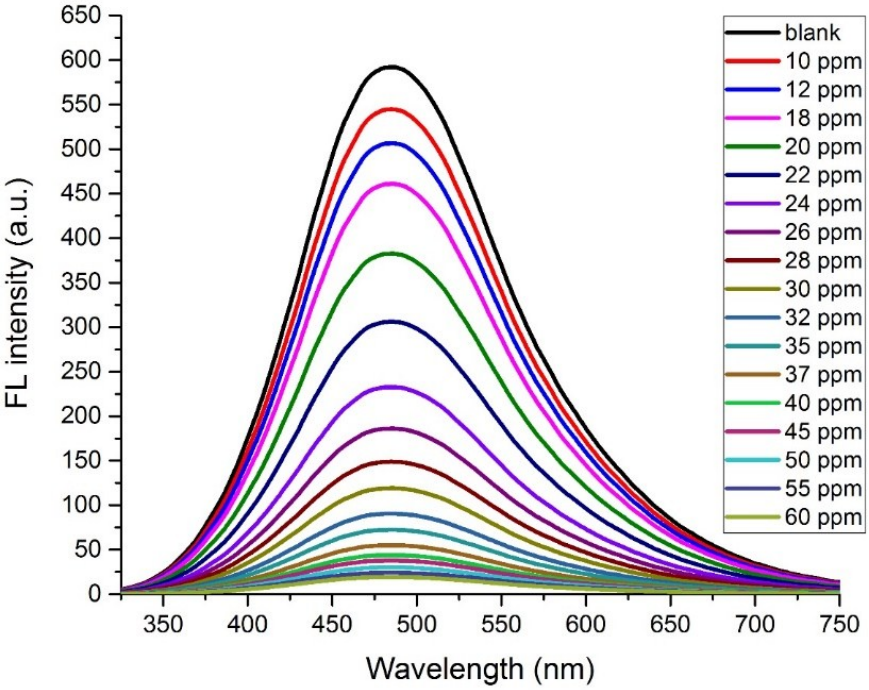

Figure **S21**. Fluorescence emission spectra of **TMU-46S** dispersed in water solution at different concentrations of Pb^{2+}, excited at 320 nm.

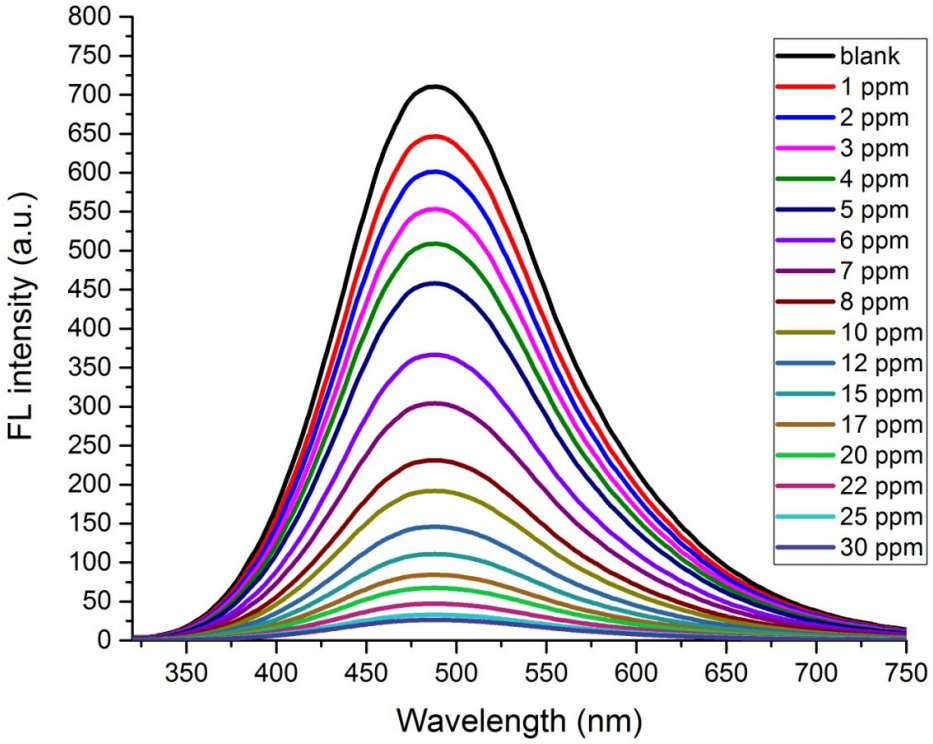

Figure **S22**. Fluorescence emission spectra of **TMU-47S** dispersed in water solution at different concentrations of $\mathbf{Hg^{2+}}$, excited at 320 nm.

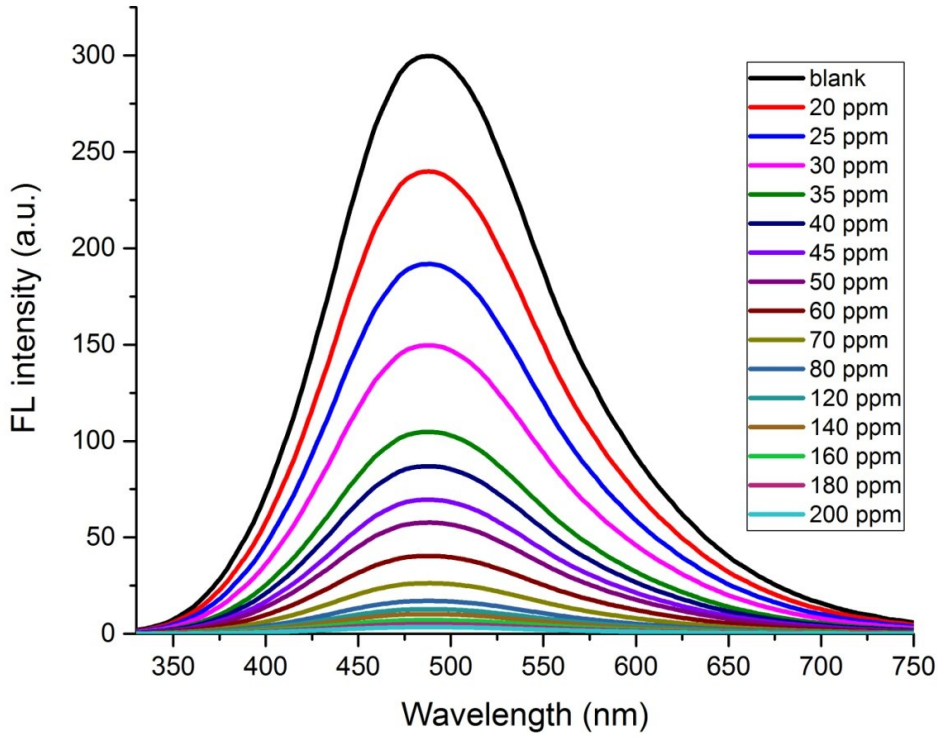

Figure **S23**. Fluorescence emission spectra of **TMU-47S** dispersed in water solution at different concentrations of $\mathbf{Ag^{+}}$, excited at 320 nm.

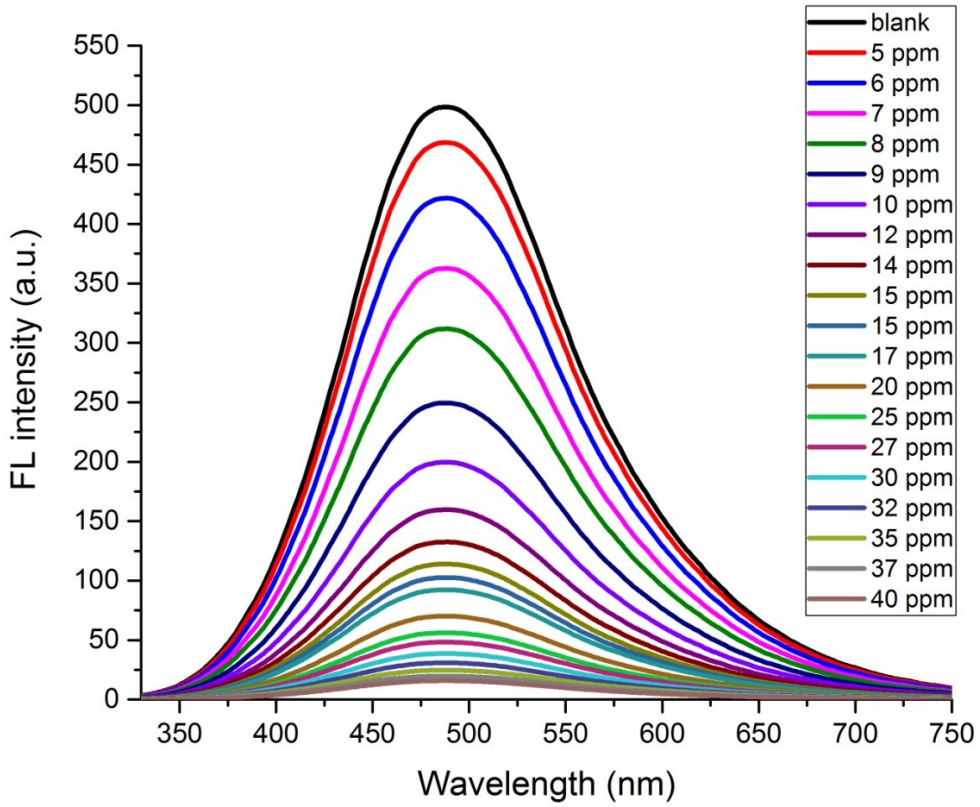

Figure **S24**. Fluorescence emission spectra of **TMU-47S** dispersed in water solution at different concentrations of $\mathbf{Pb^{2+}}$, excited at 320 nm.

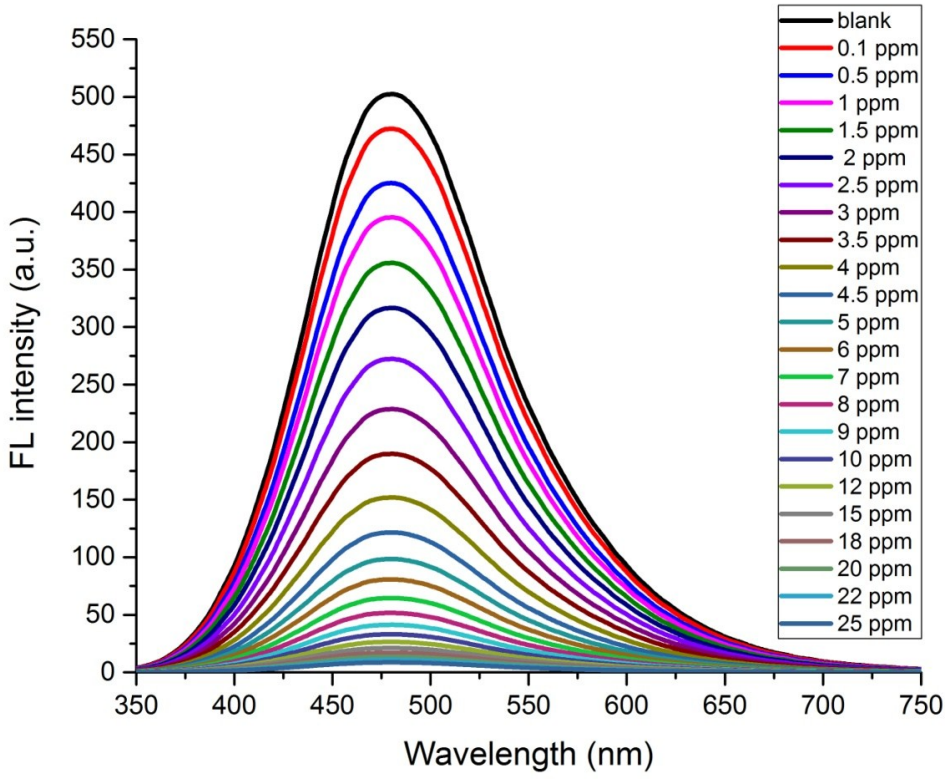

Figure **S25**. Fluorescence emission spectra of **TMU-48S** dispersed in water solution at different concentrations of Hg^{2+}, excited at 330 nm.

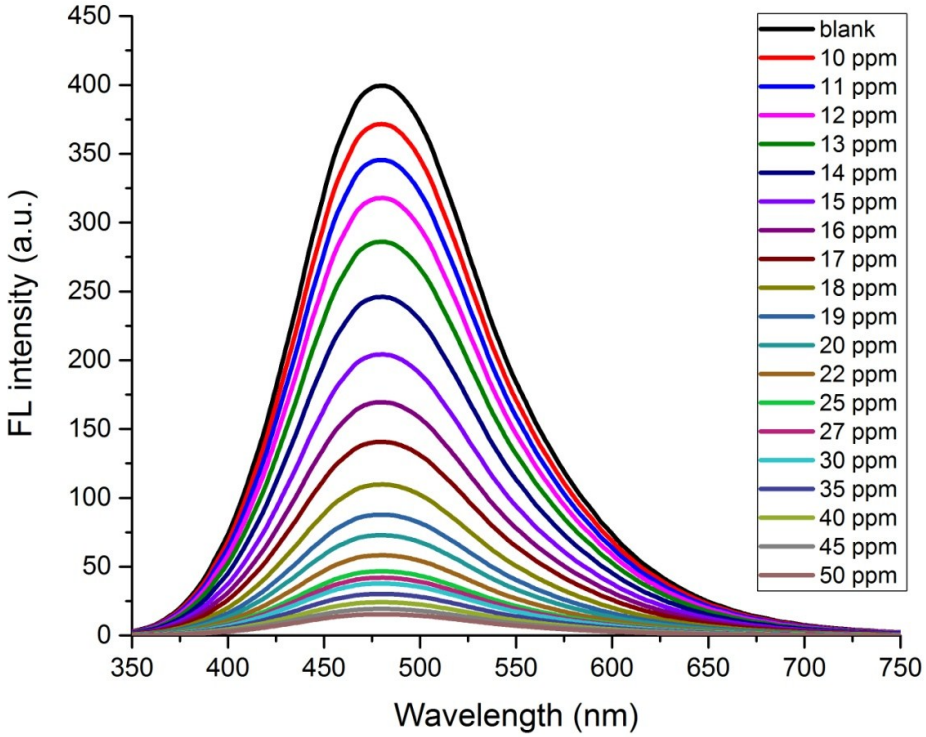

Figure **S26**. Fluorescence emission spectra of **TMU-48S** dispersed in water solution at different concentrations of Ag^{+}, excited at 330 nm.

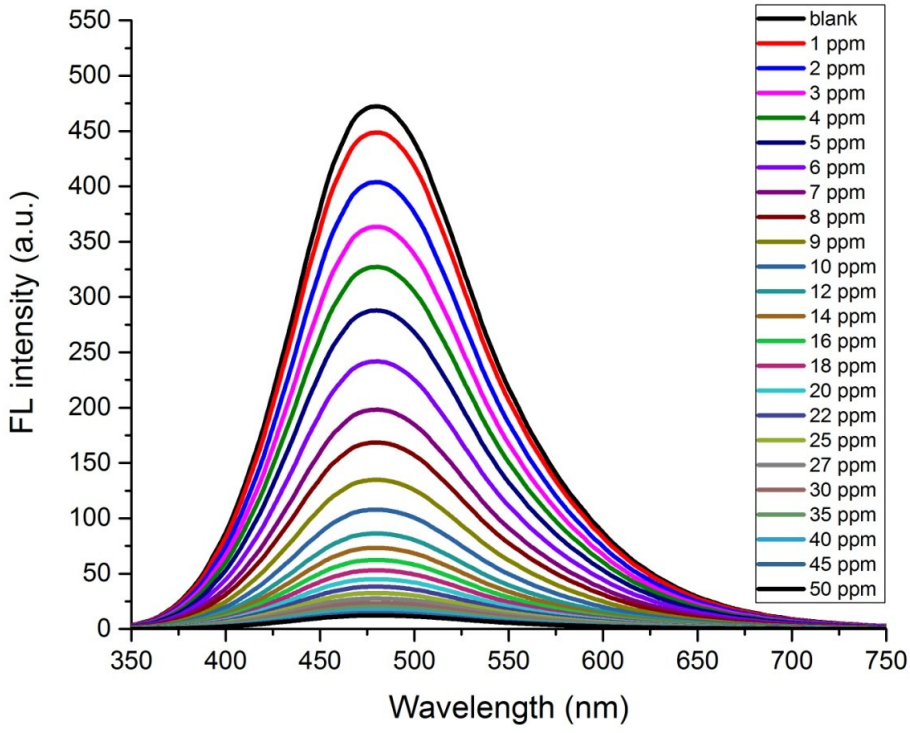

Figure **S27**. Fluorescence emission spectra of **TMU-48S** dispersed in water solution at different concentrations of Pb^{2+}, excited at 330 nm.

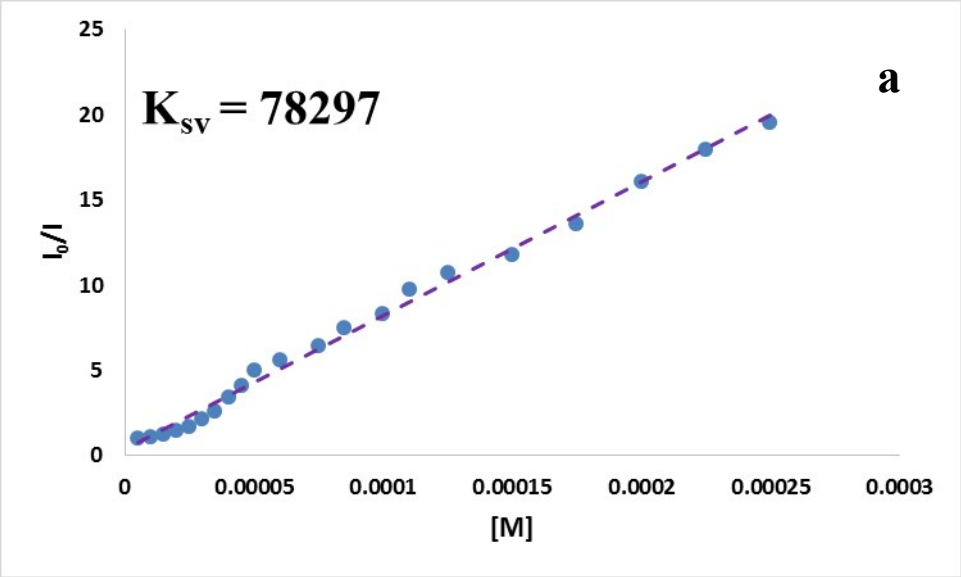
a
K_{sv} = 78297
I_0/I
25
20
15
10
5
0
0
0.00005
0.0001
0.00015
0.0002
0.00025
0.0003
[M]

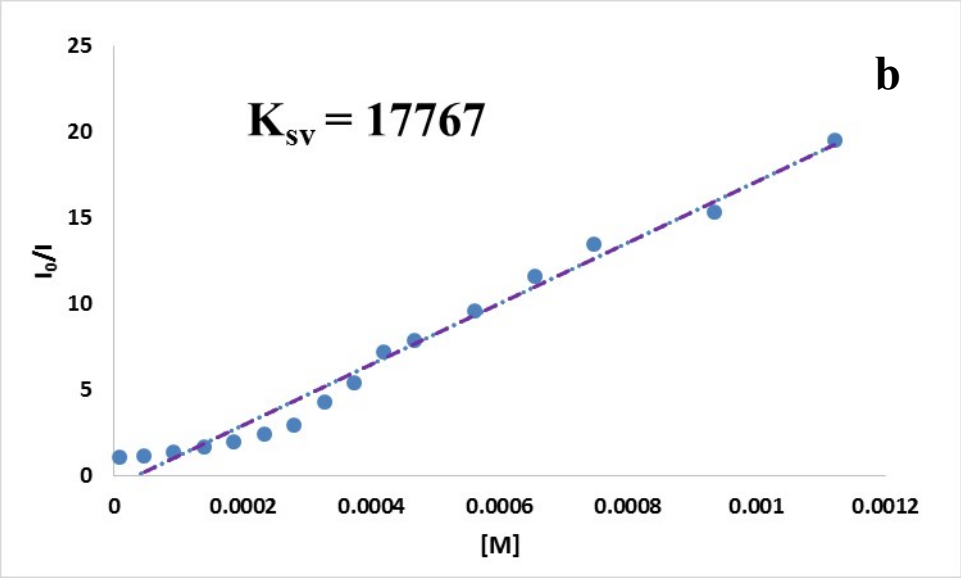
b
K_{sv} = 17767
I_0/I
25
20
15
10
5
0
0
0.0002
0.0004
0.0006
0.0008
0.001
0.0012
[M]

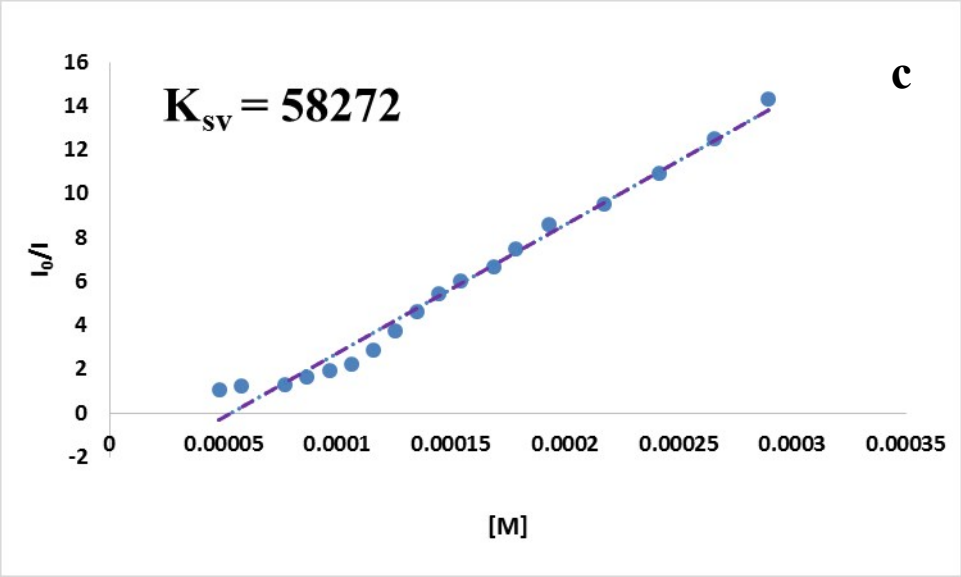

Figure **S28**. Stern–Volmer (SV) plots in the presence of 3 mg of **TMU-46S** in different Hg^{2+} (a) Ag^{+} (b) pb^{2+} (c) concentrations ([Q]) in water.

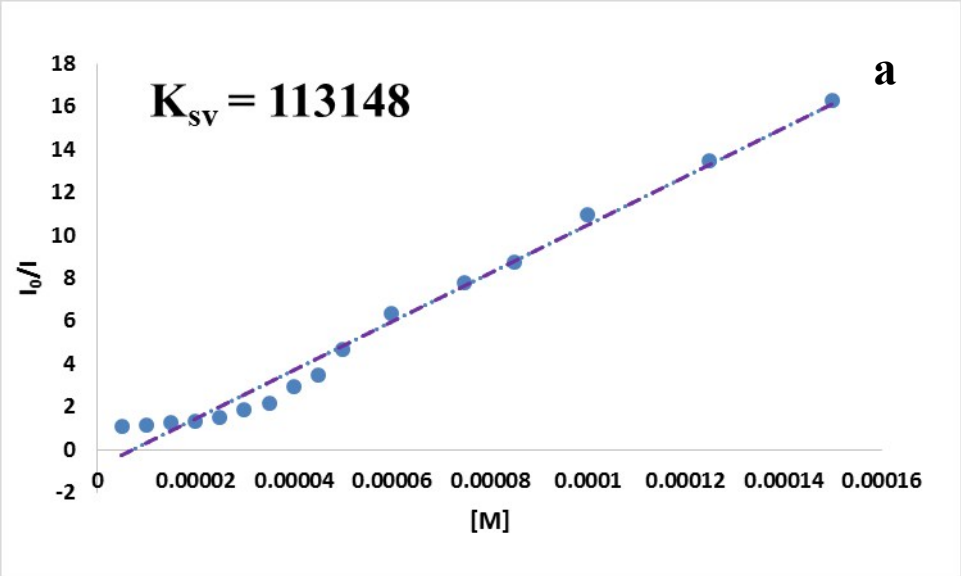

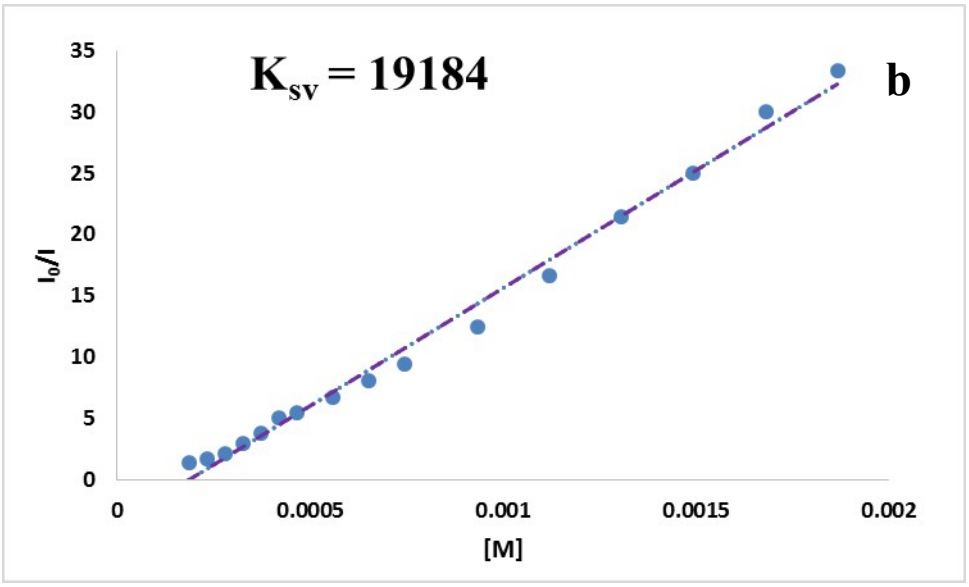

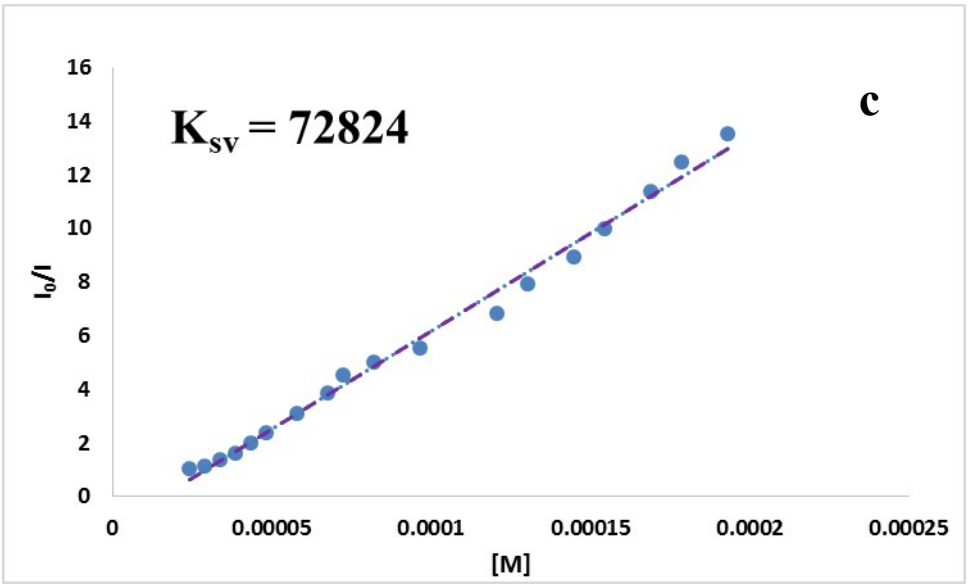

Figure **S29**. Stern–Volmer (SV) plots in the presence of 3 mg of **TMU-47S** in different **Hg^{2+}** (a) **Ag^{+}** (b) **pb^{2+}** (c) concentrations ([Q]) in water.

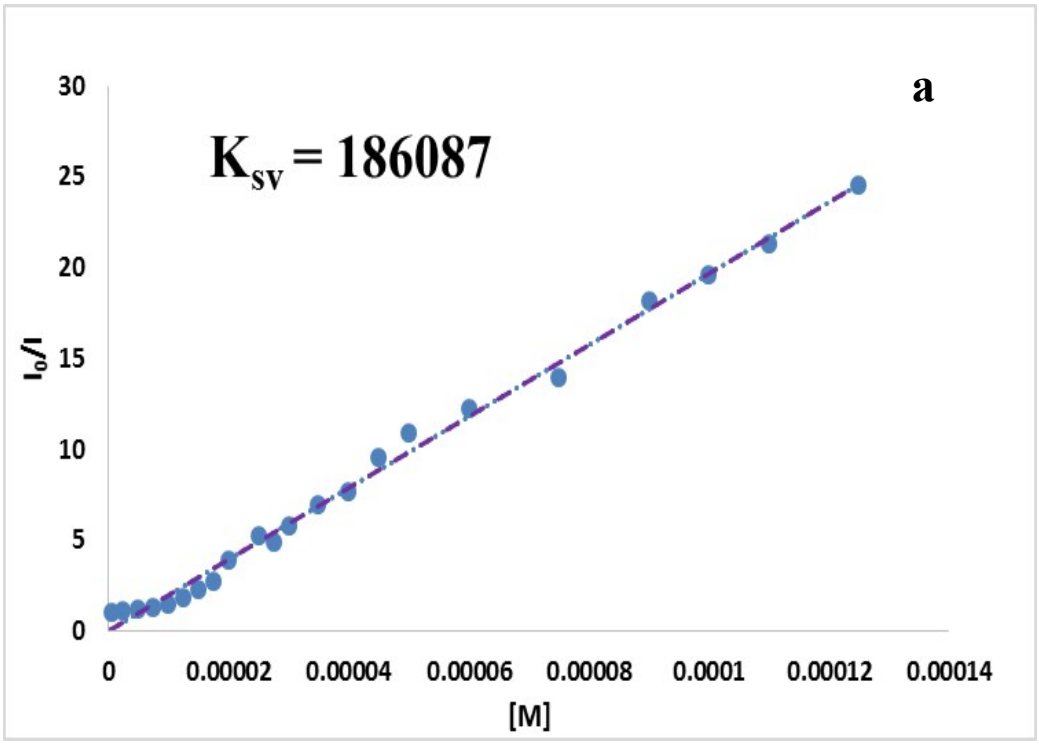
a
K_{sv} = 186087
I_0/I
30
25
20
15
10
5
0
0
0.00002
0.00004
0.00006
0.00008
0.0001
0.00012
0.00014
[M]

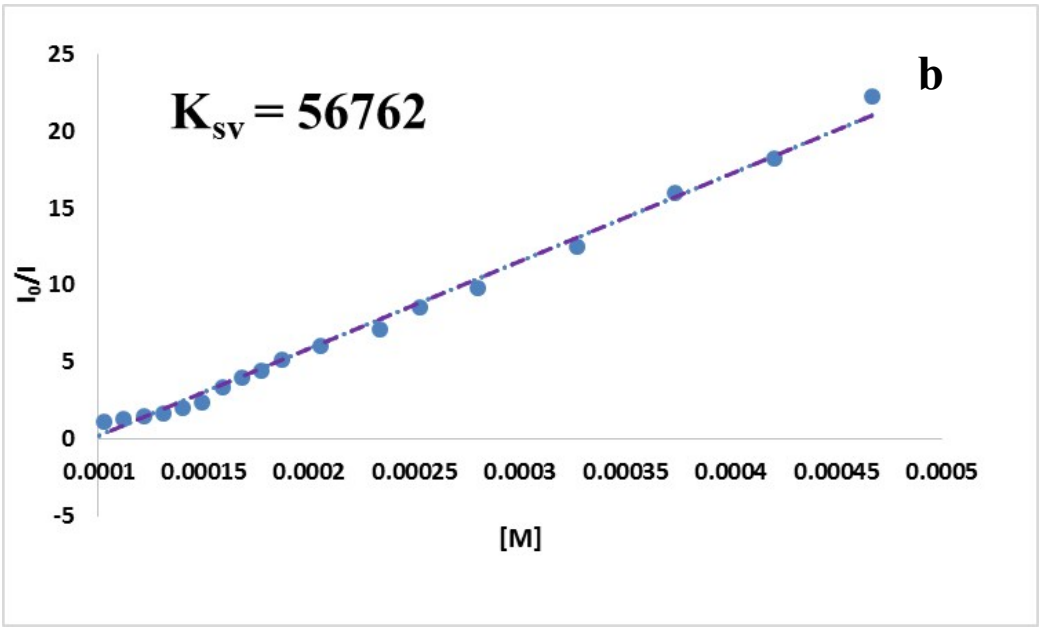
b
K_{sv} = 56762
I_0/I
25
20
15
10
5
0
-5
0.0001
0.00015
0.0002
0.00025
0.0003
0.00035
0.0004
0.00045
0.0005
[M]

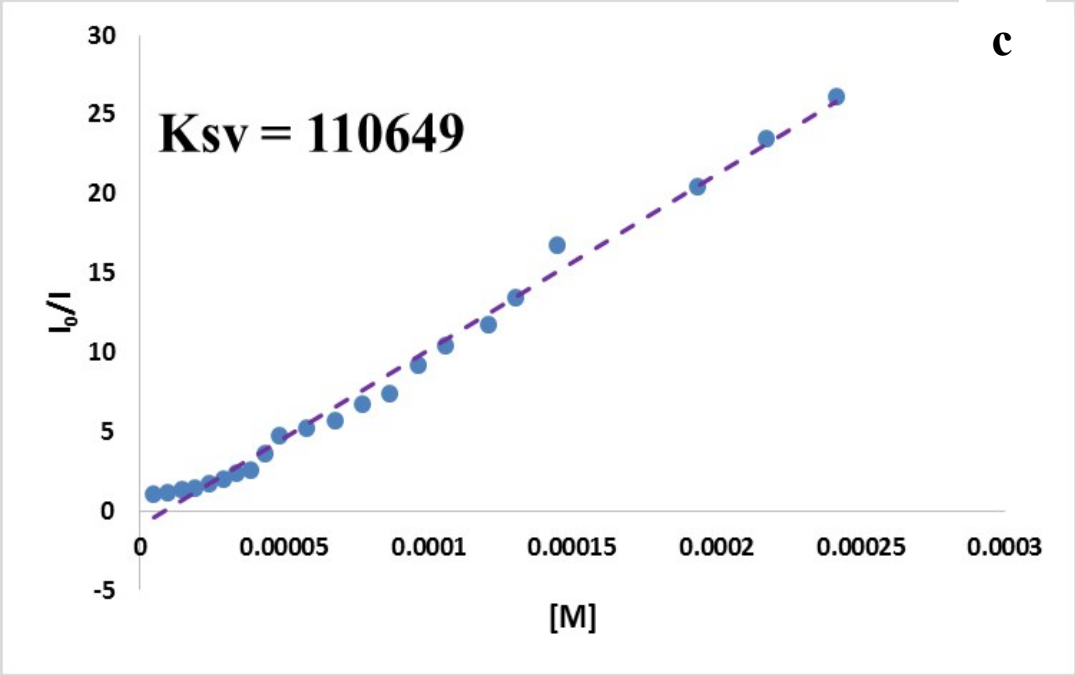

Figure **S30**. Stern–Volmer (SV) plots in the presence of 3 mg of **TMU-48S** in different $\mathbf{Hg^{2+}}$ (a) $\mathbf{Ag^{+}}$ (b) $\mathbf{pb^{2+}}$ (c) concentrations ([Q]) in water.

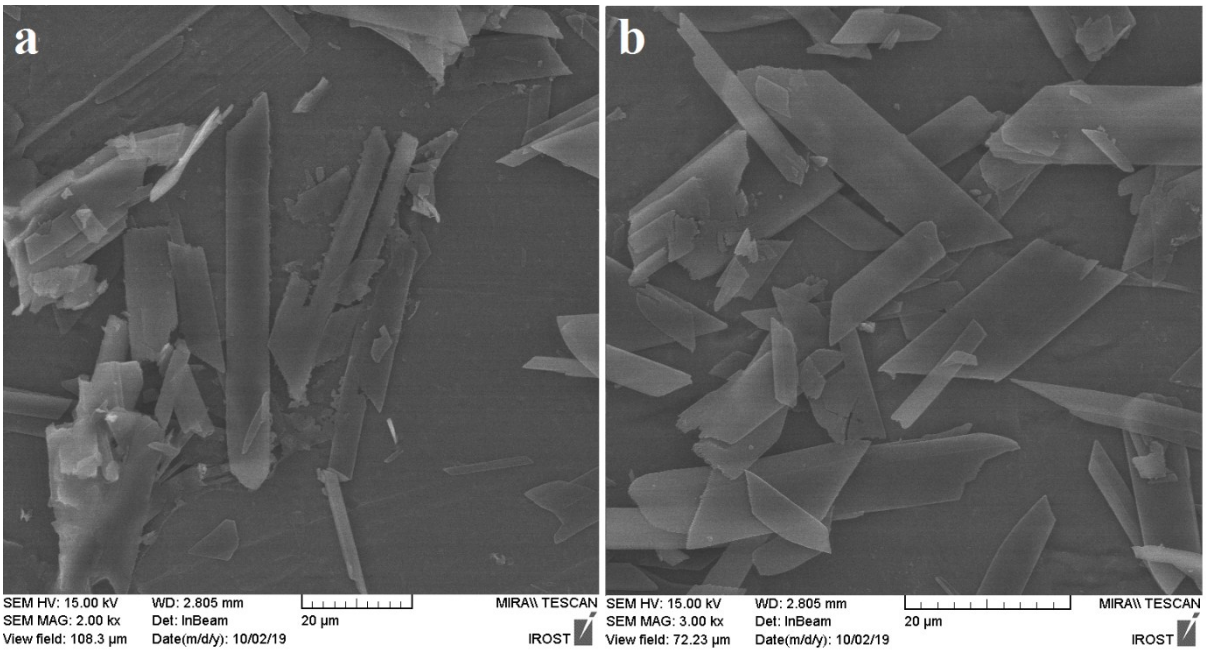

Figure **S31**. FE-SEM images of a) TMU-48S and b) TMU-48 as-synthesized particles

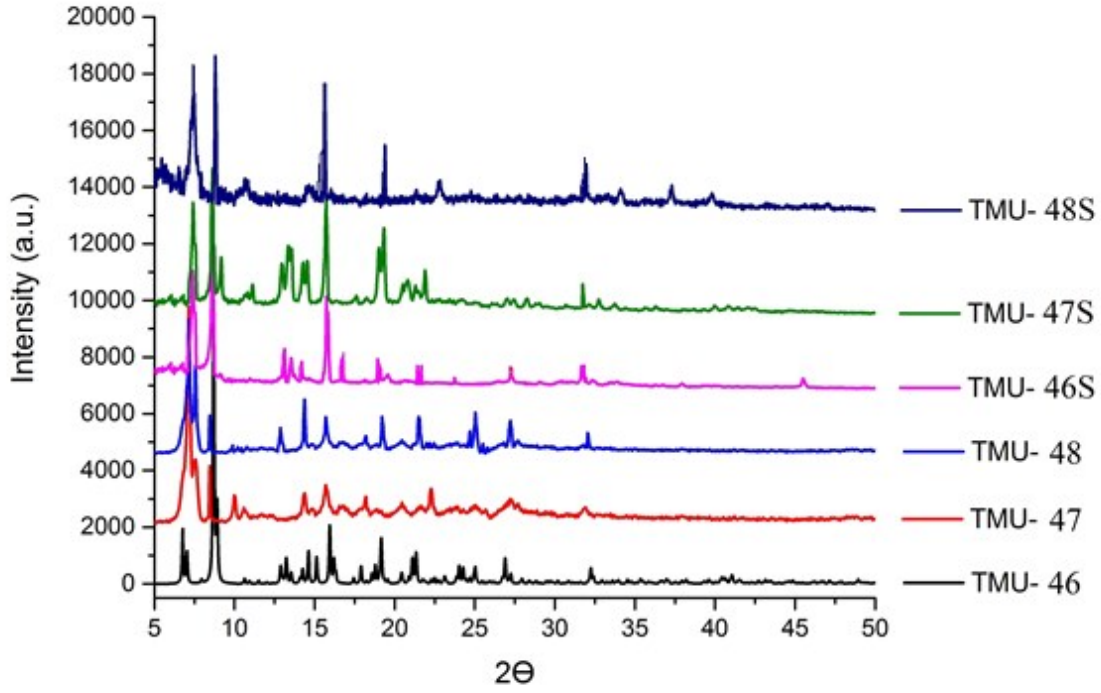

Figure **S32**. PXRD patterns of simulated and after sensing and activated form of **TMUs**

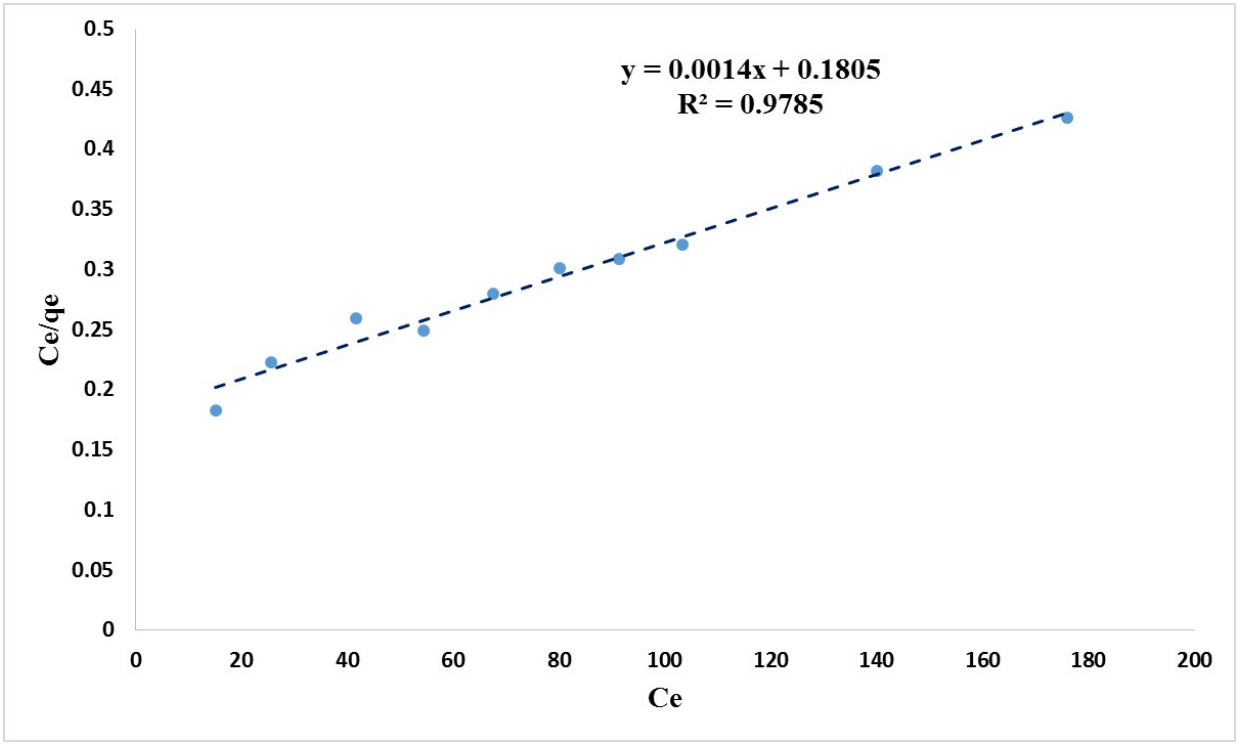

Figure **S33**. Effect of initial Hg^{+2} concentration on adsorption by 3 mg of TMU-48S

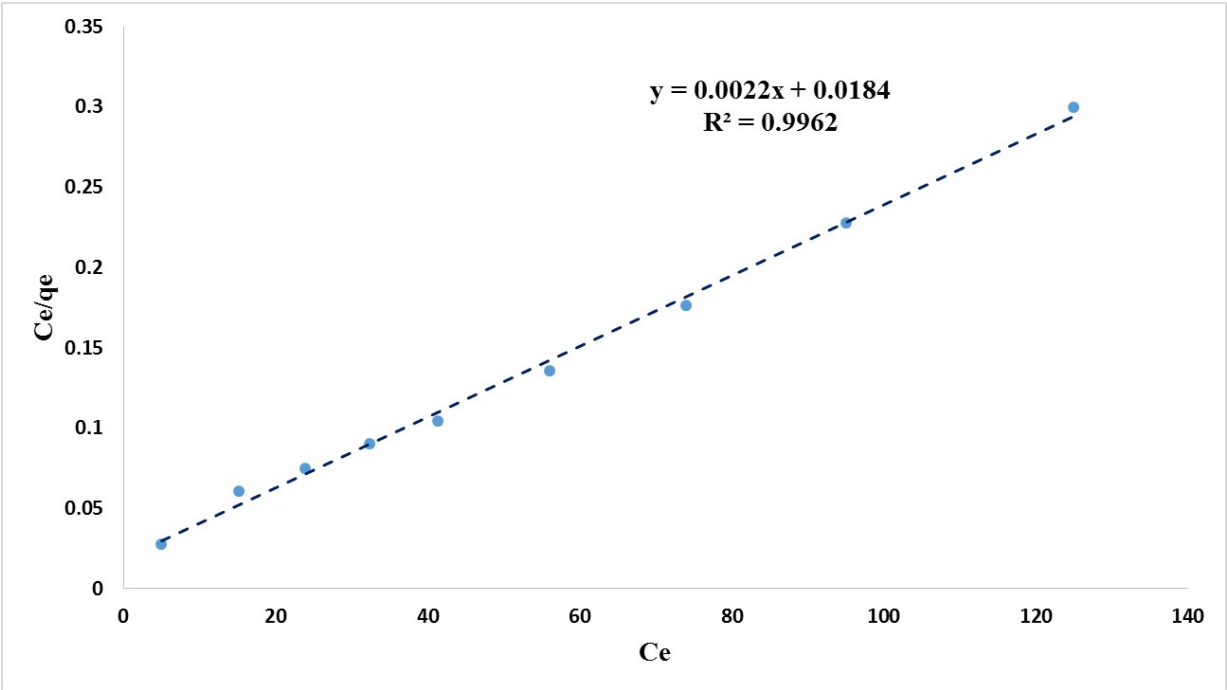

Figure **S34**. Effect of initial Pb^{+2} concentration on adsorption by 3 mg of TMU-48S

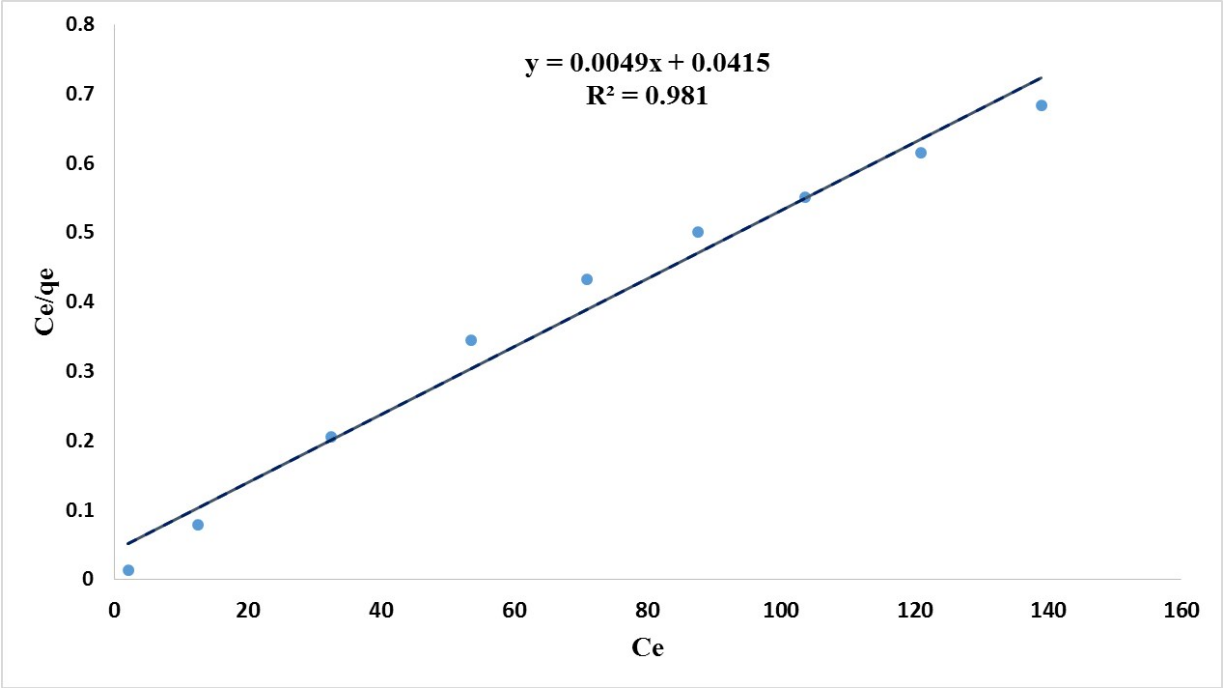

Figure **S35**. Effect of initial Ag^{+} concentration on adsorption by 3 mg of TMU-48S

Table.S3: The interaction energies ligands bpta, bpfb, bpfn and S in the presence of metal cations were studied.

		Complex	Ligand	Metal	interaction energies
Pb	**bpfb**	**-1066.74**	**-1063.87**	**-2.65346**	**-135.5**
	bpta	**-1066.74**	**-1063.87**	**-2.65346**	**-134.6**
	pbfn	**-1220.42**	**-1217.51**	**-2.65346**	**-160.6**
	S	**-875.031**	**-872.13**	**-2.65346**	**-155.3**
Hg	**bpfb**	**-1105.96**	**-1063.87**	**-41.7935**	**-191.3**
	bpta	**-1105.95**	**-1063.87**	**-41.7935**	**-178.8**
	bpfn	**-1259.62**	**-1217.51**	**-41.7935**	**-198.4**
	S	**-914.199**	**-872.13**	**-41.7935**	**-173.2**
Ag	**bpfb**	**-1209.39**	**-1063.87**	**-145.474**	**-32.7**
	bpta	**-1209.4**	**-1063.87**	**-145.474**	**-33.8**
	pbfn	**-1363.03**	**-1217.51**	**-145.474**	**-30.5**
	S	**-1017.67**	**-872.13**	**-145.474**	**-39.5**

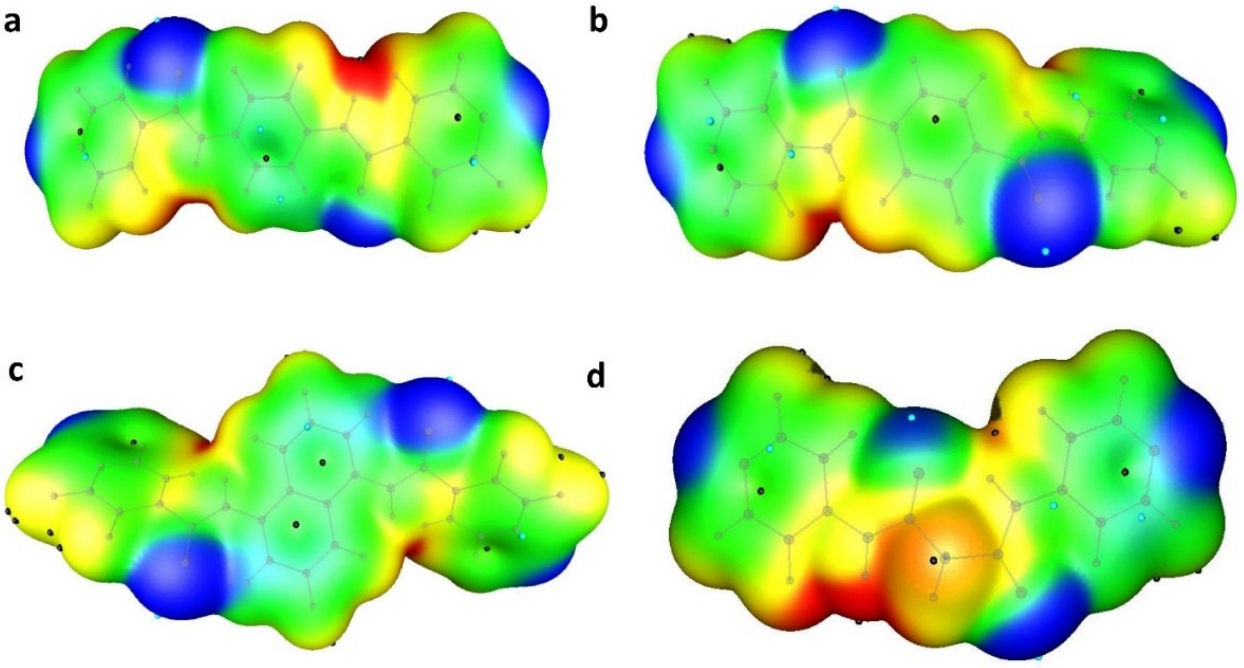

Figure **S36**: Electrostatic potentials mapped on the electron isodensity surface of ligand bpfb(a), bpta(b), bpfn(c) and S(d).The color code, in kcal/mol, is: red > 30; 30 > yellow > 15; 15 > green > 0 and blue < 0. The black and blue circles indicate the surface maxima and minima, respectively.